Lecture on Femto-Second Diagnostics

Part I: Motivation
Streak Camera
Deflecting Cavity
Coherent Radiation

Part II: Interferometric Techniques
Electro-Optical Techniques

V. Schlott (PSI)

Acknowledgements

… to be able to present a state-of-the-art overview of femto-second diagnostics, I have been relying on the outstanding work of many colleagues from various accelerator institutes (mainly XFELs)

… this presentation is far from being complete ! It tries to give an overview of fs diagnostics techniques with some – hopefully instructive – examples and (latest) measurements

… for their support in discussing the topics, which are presented, and for the provision of information and measurement results, I would like to explicitly thank the following colleagues…:

Bernd Steffen (PSI / formerly DESY)
Yoo Jong Kim (PSI)
Daniel Sütterlin (formerly PSI)
Dirk Abramsohn (formerly PSI)
Andreas Streun (PSI)
Gerhard Ingold (PSI)
Paul Beaud (PSI)

M. Metzger (Hamamatsu Photonics)

R. Fiorito (Uni Maryland)
A. Shkvarunets (Uni Maryland)

the FLASH Operations Group

the DESY FLA Group with…
Bernhard Schmidt (DESY)
Peter Schmüsser (Uni HH)
Axel Winter (DESY)
Michael Röhrs (DESY)
Florian Löhl (DESY)
Jan Menzel (formerly DESY)
Lars Fröhlich (formerly DESY)

the LCLS Commissioning Team
and…
Paul Emma (SLAC)
Dave Dowell (SLAC)
Henrik Loos (SLAC)
Joe Frisch (SLAC)

David Alesini (INFN-LNF)

and many more…!!!

Motivation for fs Diagnostics – Requirements in XFEL Accelerators

Bunch Arrival Time Monitor

τ_{Gun} < 1 ps
$\tau_{Injector}$ ~ 100 fs

beam pick-up & EO modulator
cavity and RF-mixing

Electro-Optical BL-Monitor

τ_{Bunch} ~ 10 ps - 100 fs

single-shot bunch length
(spectral & temporal decoding)
bunch arrival time

not covered in this talk…:

- Optical Replica
- Statistical Methods
- Photon Arrival Time Diagnostics
- Photon Bunch Length Diagnostics

(Diamond detectors, non-thermal melting etc…)

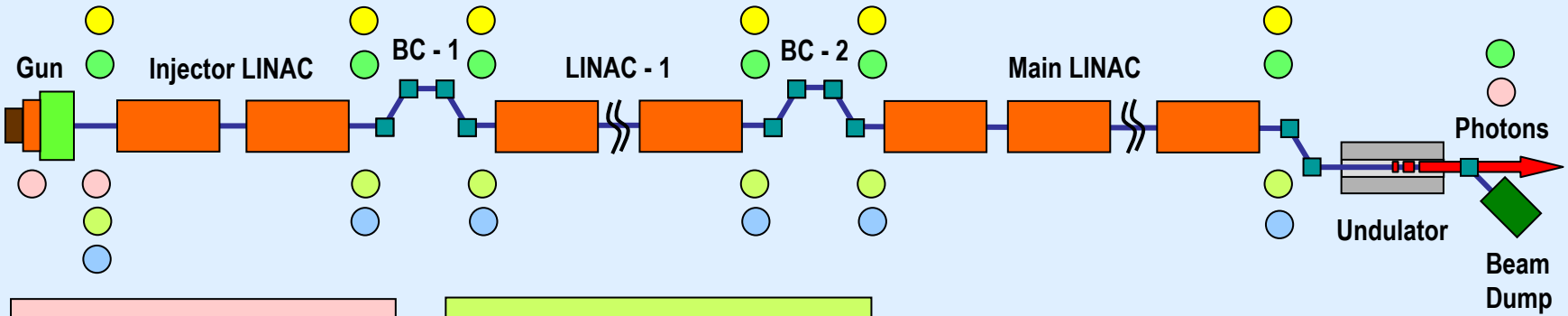

Streak Camera

τ_{Bunch} ~ 5 – 10 ps
$\tau_{RiseTime}$ ~ 500 fs

Laser diagnostics (IR, vis)
vis. Cerenkov radiation
(vis. transition radiation)

Coherent Radiation

τ_{Bunch} ~ 10 ps - 10 fs

bunching diagnostics
bunch length interferometers
single-shot EO bunch length
single-shot "poly-chromator"

Transverse RF Deflector

τ_{Bunch} ~ 5 ps - 10 fs

single-shot bunch length
"sliced" energy spread
"sliced" emittance

Streak Camera – Operating Principle

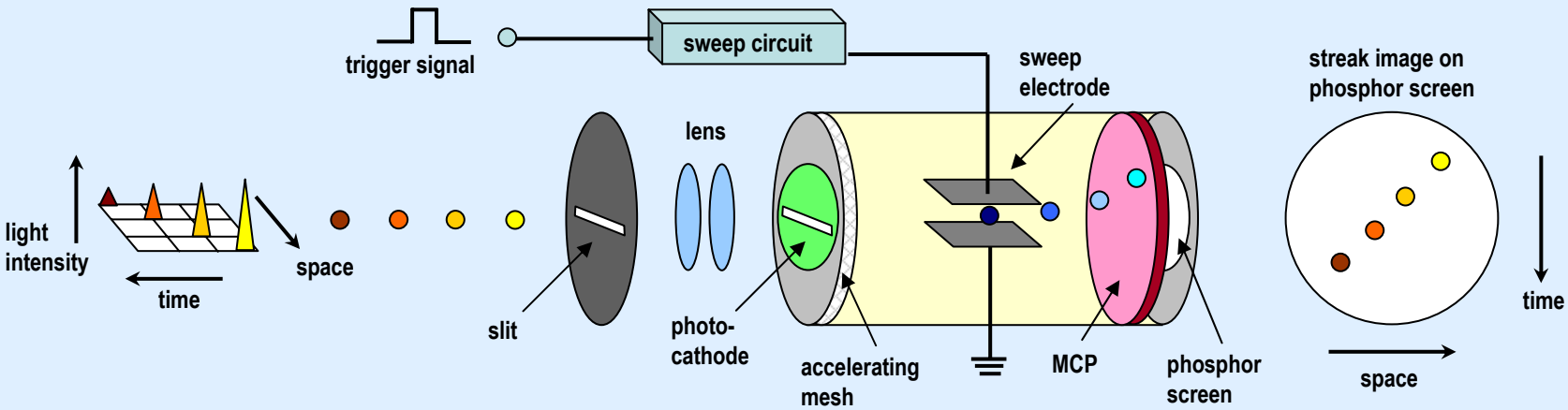

- visible light pulses (e.g.: Cerenkov radiation, optical transition radiation or synchrotron radiation) are converted on the photo-cathode into a number of electrons, which are proportional to the incident intensity distribution
- the photo-electrons are accelerated along the streak tube, transversely (vertically) swept by deflecting plates to convert the incident time distribution in a spatial distribution on the MCP
- the photo-electrons are amplified by the MCP and converted back to visible light on the phosphor screen
- an initial spatial offset of the light pulses at the entrance slit is preserved at the phosphor screen

Streak Camera – Limitations of Time Resolution (for Hamamatsu FESCA-200)

- streak camera time resolution is limited by *transit spread* and *temporal spread* of photo-electrons

- *transit spread* for FESCA-200 is given by:

$$\tau_S = 2.34 \cdot 10^{-6} \cdot (\Delta E)^{1/2} / E$$

with accelerating electric field $E = 9.4 \cdot 10^6$ V/m
and photo electron energy distribution ΔE (see graph for S-20 photocathode)

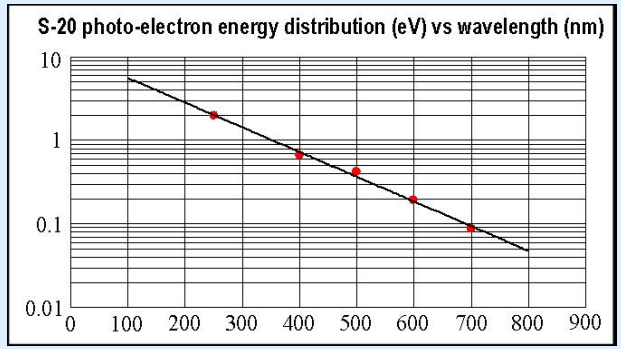

courtesy of Hamamatsu Photonics

- *temporal spread* for FESCA-200 is given by:

$$\tau_F = w / v = 0.152 \cdot 10^{-12} \text{ s}$$

with non-deflected line spread $w = 60 \cdot 10^{-6}$ m
and sweep speed $v = 3.96 \cdot 10^8$ ms^{-1}

FESCA-200 time resolution…

only measured / guaranteed time resolution
below 300 fs at 800 nm incident light wavelength

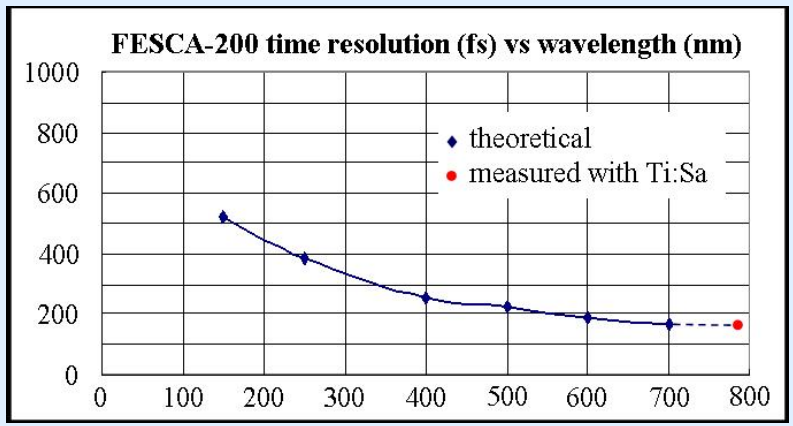

courtesy of Hamamatsu Photonics

Example of fs Streak Camera Measurement at an Accelerator

taken from *"T. Watanabe et al. / Nuclear Instruments and Methods in Physics Research A 480 (2002) 315–327"*

- **streak camera (FESCA-200) images were taken at 35 MeV beam energy behind University of Tokyo LINAC using visible Cerenkov radiation in air**
- **three set-ups with different optical band-pass filters were used to examine influence on time resolution:**
  - ○ **lens optics for light transport and SC imaging system**
  - ● **lens optics for light transport and mirror optics for SC imaging system**
  - ♦ **mirror optics for both, light transport and SC imaging system**

FESCA-200 measurements of Cerenkov light for different optical set-ups

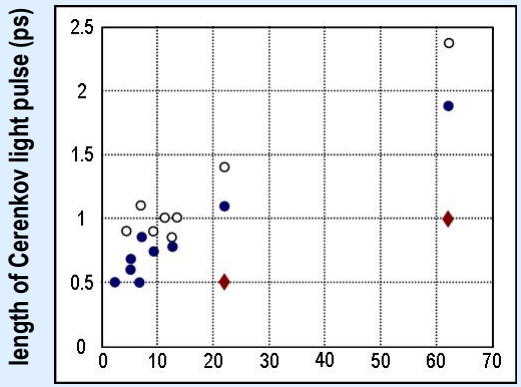

Schematic Layout for Lens Optics

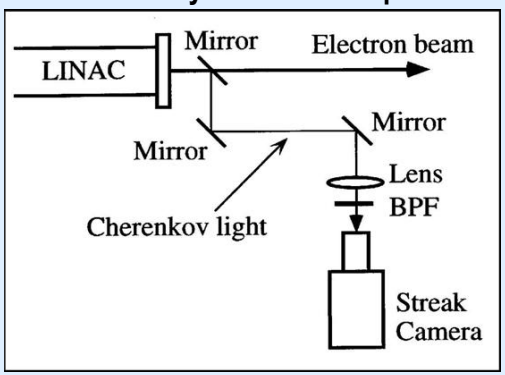

Schematic Layout for Mirror Optics

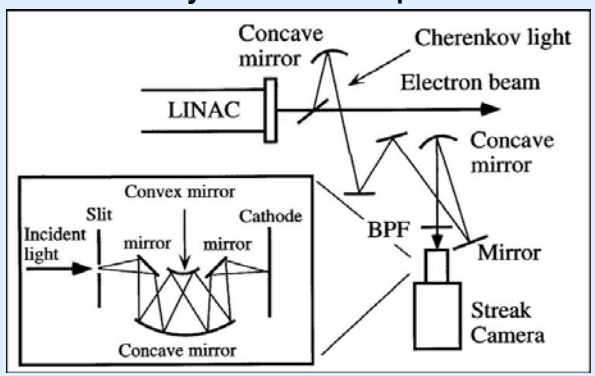

FESCA-200 streak image of Cerenkov light

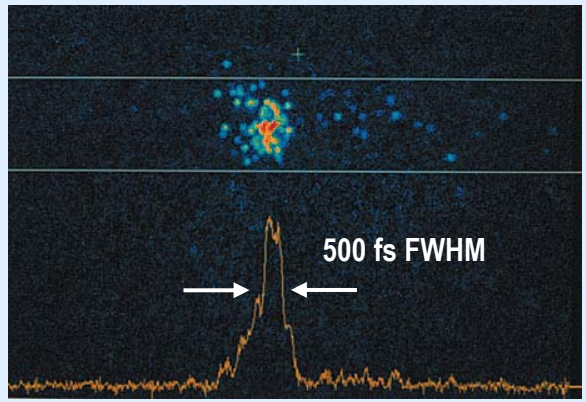

all images are courtesy of T. Wanatabe et al. (Uni Tokyo)

Example of fs Streak Camera Measurement at an Accelerator

many thanks to D. Dowell, P. Emma and the LCLS commissioning team! See also: PR-STAB 11 30703 (2008) about LCLS injector commissioning and D. Dowell et al., Proc. PAC'07, p. 1317 (TUPMS058)

Streak Camera and XCorr Images – LCLS Gun Laser Pulse

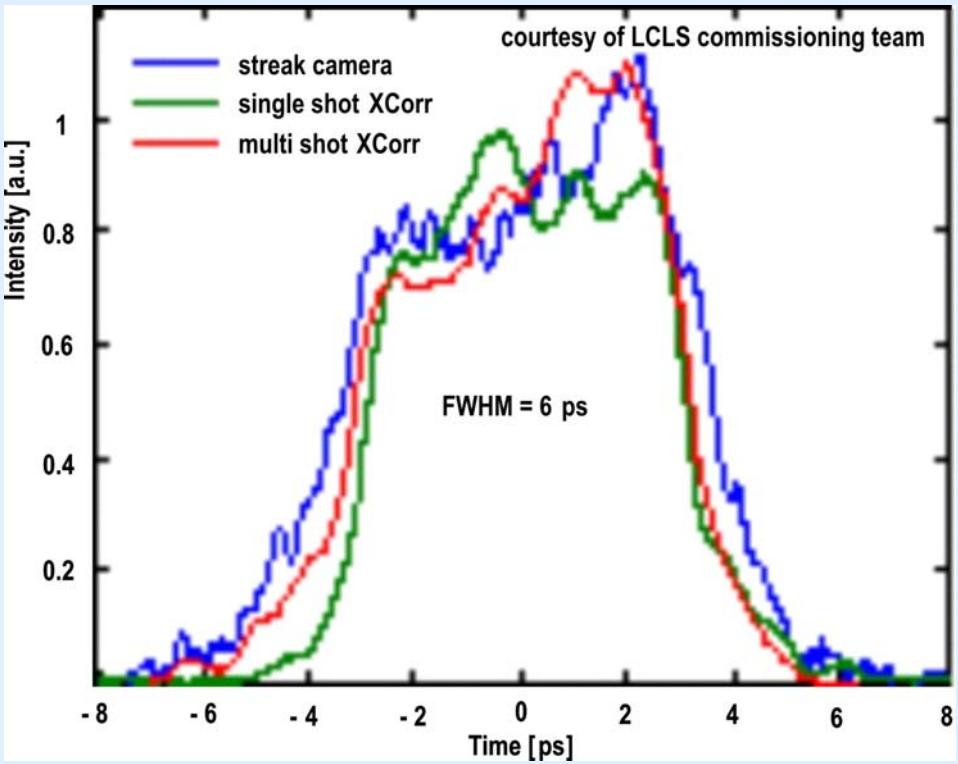

Image taken from: D. Dowell et al., Proc. PAC'07, p. 1317 (TUPMS058)

Optimization using XCorr in the UV

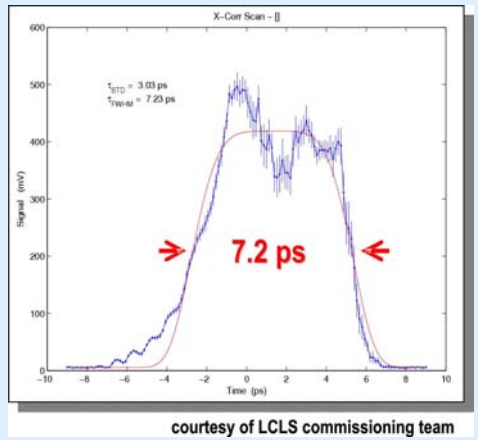

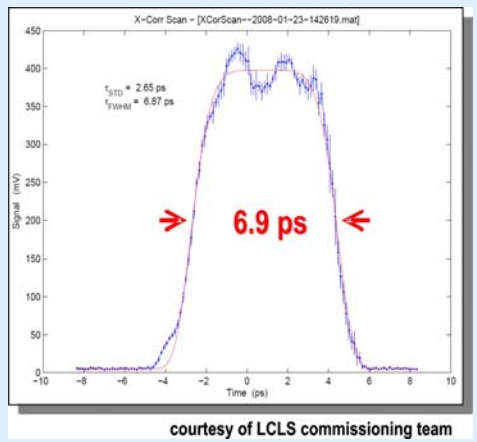

Streak Camera for fs Diagnostics – Summary

- streak cameras are useful and intuitive instrumentation to measure and optimize laser and electron beam bunch lengths and longitudinal bunch structures with ps and sub-ps time resolution
- the streak camera time resolution strongly depends on (is limited by)…:
  - the photon energy (wavelength) of the incoming light (preferably 600 – 800 nm for S20 photo-cathode) and the related energy spread of the photo electrons, produced at the photo-cathode of the streak tube
  - the bandwidth of the incoming light (10 nm – 20 nm band-pass filters should be used)
  - dispersion of the streak cameras in-coupling optics
- when using broad-band radiation sources like Cerenkov, transition or synchrotron radiation for electron beam diagnostics, fs time resolution can only be obtained with dispersion-free (mirror) optics for transferring light to the streak camera
- fs streak cameras are very useful instrumentation for… (personal opinion):
  - photo-gun laser diagnostics in order to verify longitudinal bunch shaping (rectangular bunch shapes)
  - low energy electron bunch length diagnostics (using Cerenkov radiation)
  - high repetition (MHz) rate bunch length measurements (using synchro-scan options)
  - on the experimental side as fast X-ray detectors (see: fs X-ray streak camera development programs)
- streak cameras are rarely used as online bunch length diagnostics, since they are usually not providing signals, which can be used in an automated feedback loop

Streak Camera Development as sub-ps Experimental X-Ray Detector

Sub-ps X-ray streak camera system as presently developed by Maik Kaiser at PSI (SLS) – present time resolution ~1 ps

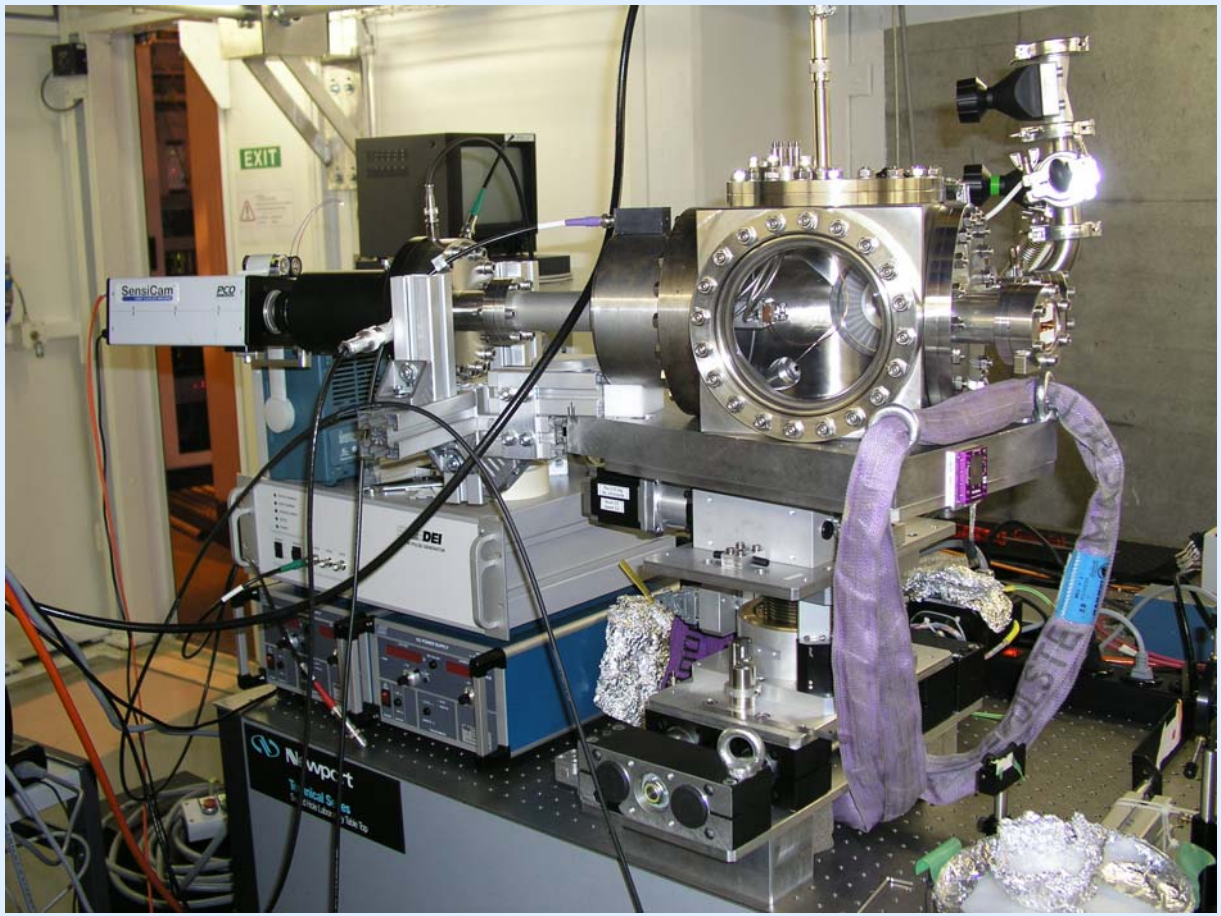

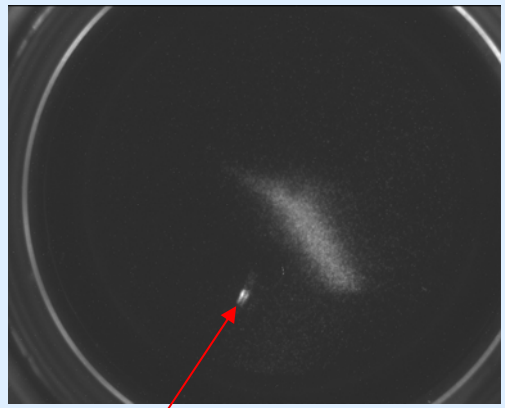

streak image of UV laser pulses separated by 2 ps

above: hard X-ray pulse from SLS X05DA bending magnet

Gaussian fit to the line readout

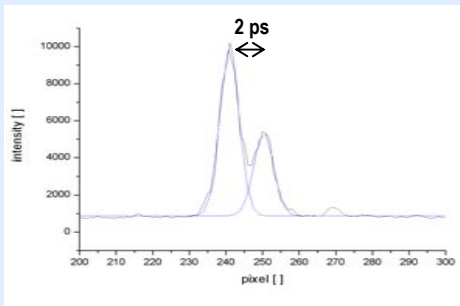

TW and SW Transverse RF Deflecting Structures

- **Iris-loaded RF waveguide structures have been designed to provide so called *hybrid* deflecting modes ($HEM_{1,1}$) which are a linear combination of $TM_{1,1}$ and $TE_{1,1}$ dipole modes to impart transverse forces to synchronously moving relativistic particle beams → *beam separators, RF deflectors***

Traveling Wave "LOLA-type" RF deflector (SLAC-design)

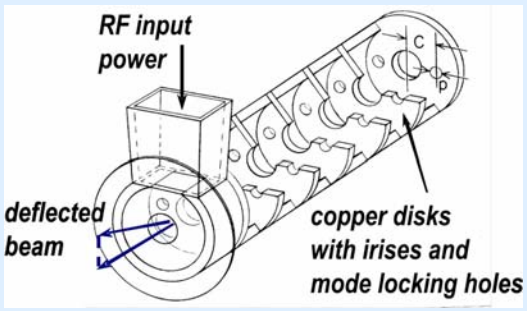

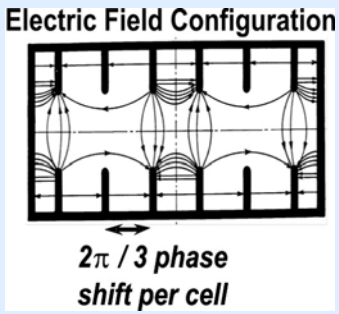

"LOLA" deflectors have been named after their inventors:
G.A. *Lo*ew, R.R. *L*arsen, O.A. *A*ltenmueller (SLAC – 1960's)

"LOLA" (TW-structure) maximum deflecting voltage:

$$V_T \approx 1.6\left[\frac{MV}{m\cdot\sqrt{MW}}\right]\cdot L[m]\cdot\sqrt{P[MW]}$$

Relation found analytically and confirmed experimentally

Standing Wave RF deflector (SPARC – INFN design)

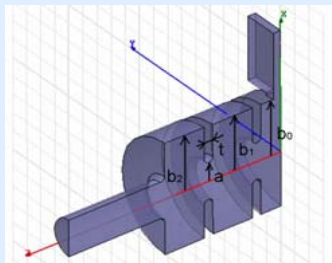

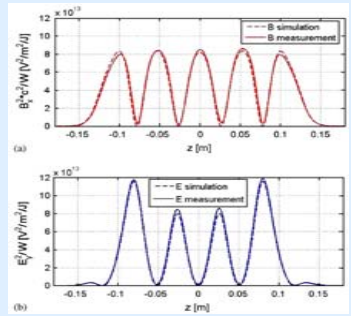

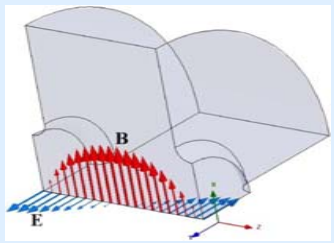

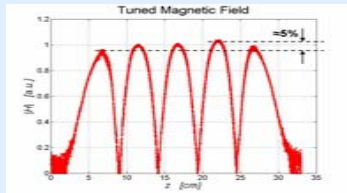

courtesy of David Alesini (INFN-LNF)
pictures taken from NIM-A 568 (2006) 488 and PAC'07 – FRPMN030, p. 3994

SPARC-type (SW-structure) max. deflecting voltage:

$$V_T\,[MV] \approx \sqrt{2\cdot P[MW]\cdot R_S\,[M\Omega]}$$

with shunt impedance R_S ~ 0.5 MΩ · number of cells

Transverse RF Deflecting Structures – LCLS, FLASH & SPARC

Low Energy TW LOLA-type RF Deflector @ LCLS

TW LOLA-type RF Deflector @ FLASH

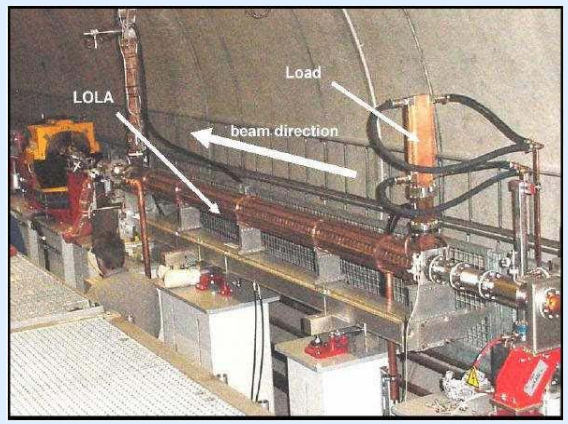

High Energy TW LOLA-type RF Deflector @ LCLS

Standing Wave RF Deflector @ SPARC - INFN

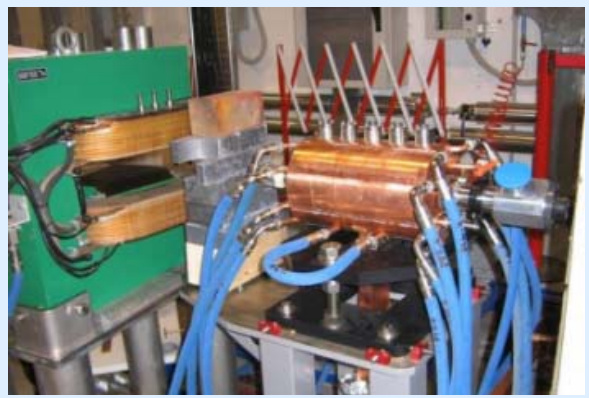

Principle of Bunch Length Measurement with RF Deflector

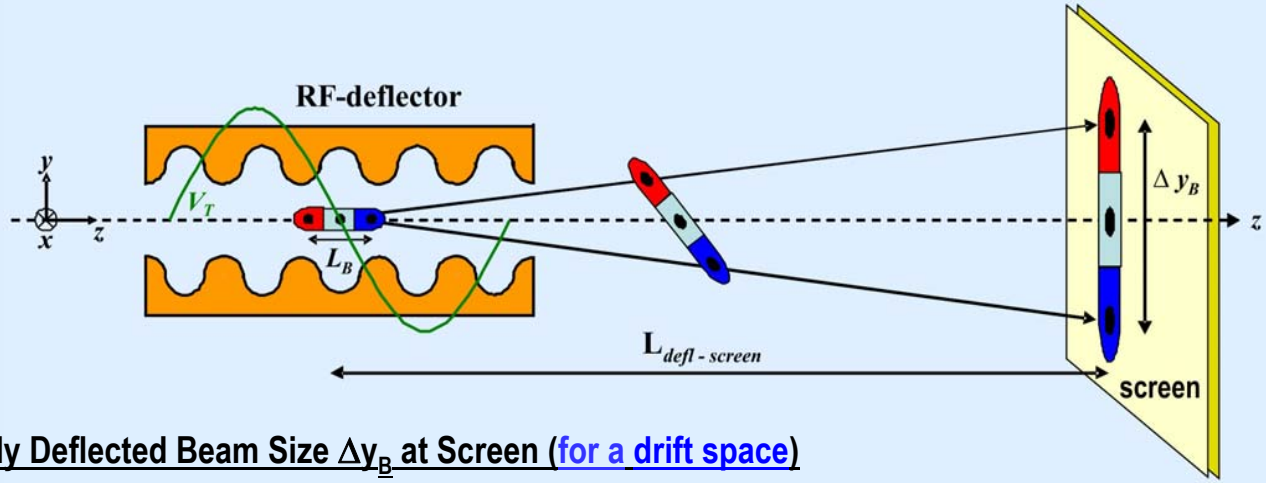

Transversely Deflected Beam Size Δy_B at Screen (for a drift space)

$$\Delta y_B = \frac{\omega_{RF} V_T}{2c\,E/e} \cos(\varphi_{RF})\; L_B\; \Delta L_{def-screen}$$

Assuming…:

- φ_{RF} = 0° at the center of the bunch results in shearing of particle density distribution without changing mean particle position
- longitudinal stability (bunch arrival time vs. RF phase) must be high in case of averaging of measurements
- pencil-like beam (zero-emittance)
- no beam offset in the RF deflector

Example:

Parameters for 250 MeV PSI FEL Injector Test Facility

ω_{RF}	=	$2\pi \cdot 3$	GHz
V_T	=	2.5	MV
c	=	$3 \cdot 10^8$	ms^{-1}
E	=	250	MeV
L_B (FWHM)	=	600	fs
	=	200	μm
$\Delta L_{def-screen}$	=	12.25	m
Δy_B	=	770	μm

Principle of Bunch Length Measurement with RF Deflector

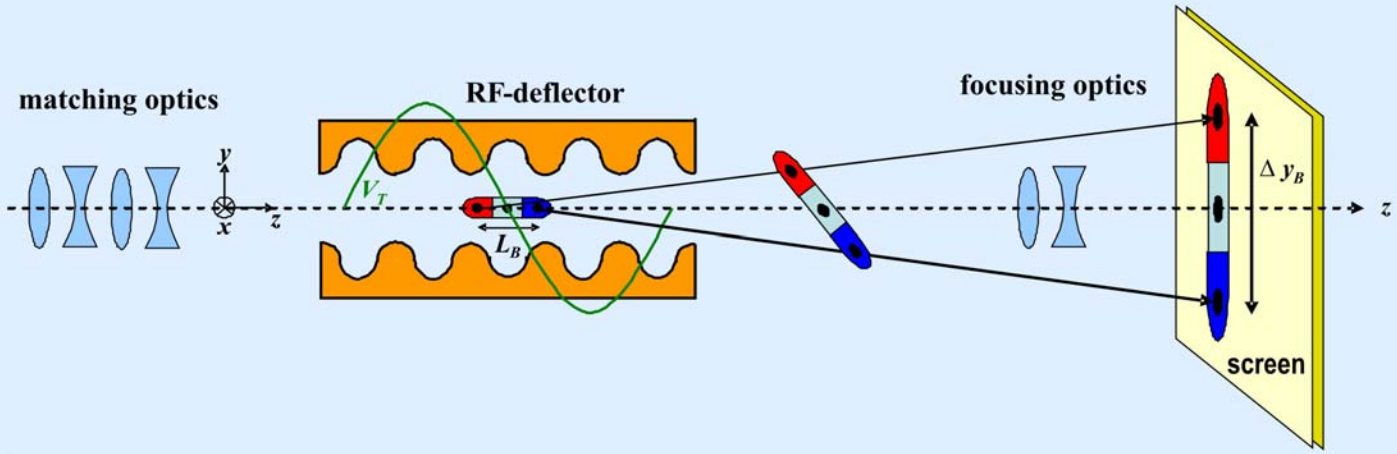

Beam Size Δy_B at Screen (vertical deflection – including beam optics)

$$\Delta y_B \underset{\lambda_{RF} >> L_B}{\cong} \frac{\omega_{RF} V_T}{2c\,E/e} L_B \cos(\varphi_{RF}) \sqrt{\beta_{y-def}\,\beta_{y-screen}} \sin(\Delta\Phi)$$

β_{y-def}	should be as large as possible for most effective kick
$\beta_{y-screen}$	should be as small as possible to increase resolution
$\Delta\Phi$	ideally 90° or 270°
$\Delta L_{def-screen}$	depends mainly on optics (phase advance between RF deflector and screen)

Example (from PSI FEL Injector Test Facility)

ω_{RF}	=	$2\pi \cdot 3$	GHz
V_T	=	2.5	MV
c	=	$3 \cdot 10^8$	ms^{-1}
E	=	250	MeV
L_B	=	600	fs
	=	200	μm
β_{y-def}	=	40	m
$\beta_{y-screen}$	=	5	m
$\Delta\Phi$	=	60	°
$\Delta L_{def-screen}$	=	3.5	m
Δy_B	=	770	μm

Bunch Length Measurement with RF Deflector - Resolution

resolution considering finite emittance ε and beam size σ

$$\sigma_{y-screen,\varepsilon} = \sqrt{\sigma_{y-def}^2 + \sigma_{y-screen}^2}$$

$$= \sqrt{\frac{\varepsilon_N \cdot \beta}{\gamma} + \left[\frac{eV_T}{E}\sigma_z\left(\frac{\omega_{RF}}{c}\cos\varphi_{RF}\right)\cdot\sqrt{\beta_{def}\,\beta_{screen}}\cdot\sin\Delta\Phi\right]^2}$$

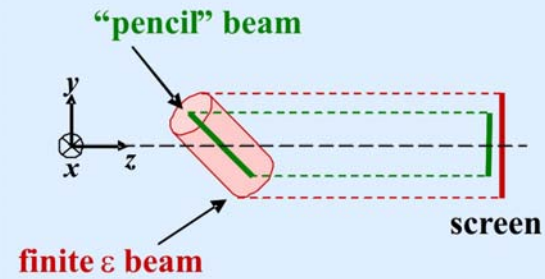

resolution limit: **deflected spot size** equals the **un-deflected beam size** $\sigma_{y\text{-screen}}$ taking finite ε into account

→ **finite ε beam size at the screen (for PSI FEL with anticipated ε_N of 0.4 μmrad)**

$$\sigma_{y-screen,\varepsilon} = \sqrt{\frac{\varepsilon_N \cdot \beta_{screen}}{\gamma}} = \sqrt{\frac{4\cdot10^{-7}\,mrad\cdot5m}{500}} = \sqrt{4\cdot10^{-9}\,m^2} \approx 65\,\mu m$$

the optical resolution should be better than the "resolution limit" given by the spot size of the finite ε beam

→ "*resolution length*" for a drift space (12.5 m)

$$L_{res} = \frac{c\,E/e}{\omega_{RF}\cdot V_T\cdot L_{drift}}\cdot\sigma_{y-screen} \approx 8.5\,\mu m \cong 28\,fs$$

→ "*resolution length*" for "PSI FEL beam optics"

$$L_{res} = \frac{c\,E/e}{\omega_{RF}\cdot V_T}\cdot\frac{\sqrt{\varepsilon_{N,y}/\gamma}}{\sqrt{\beta_{y-def}}\cdot\sin\Delta\Phi} \approx 8.5\,\mu m \approx 28\,fs$$

Time Calibration of Transverse RF Deflector – LCLS and FLASH

many thanks to Paul Emma and the LCLS commissioning team! See also: PR-STAB 11 30703 (2008) about LCLS injector commissioning
many thanks also to Michael Roehrs and the FLASH operations team! See also: Michael Roehrs, DESY-thesis May 2008

Calibration Method of Transverse RF Deflector

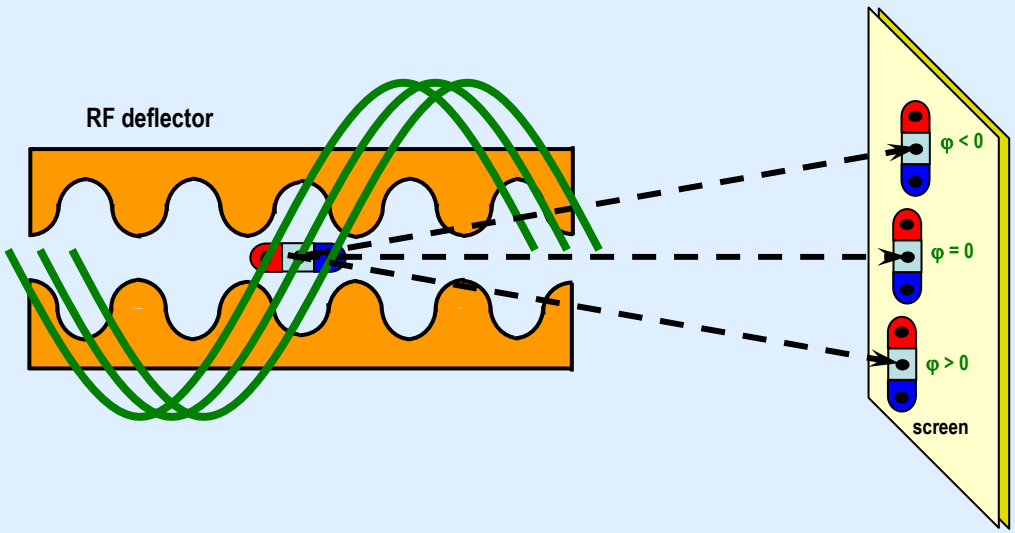

- variation of the RF phase around the "zero-crossing" of the deflecting force results in a vertical beam offset on the screen
- a calibration of RF phase $\Delta\phi$ resp. time delay Δt and beam excursion Δy can be derived in pixel / ° RF phase or mm / ps

LCLS RF deflector calibration curve (pixel vs. RF phase)

Calibration: 24.5 pixel / ° RF @ 2856 MHz ~ 45 fs / pixel

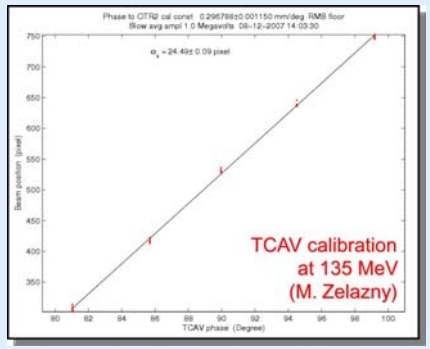

FLASH RF deflector calibration (mm vs. RF phase (time))

Calibration: ~ 42 mm / ps

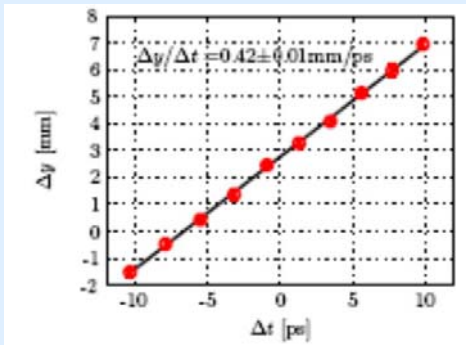

courtesy of M. Roehrs (DESY)

Examples of Bunch Length Measurement with RF Deflector – LCLS

many thanks to Paul Emma and the LCLS commissioning team! See also: PR-STAB 11 30703 (2008) about LCLS injector commissioning

Low Energy RF Deflector off

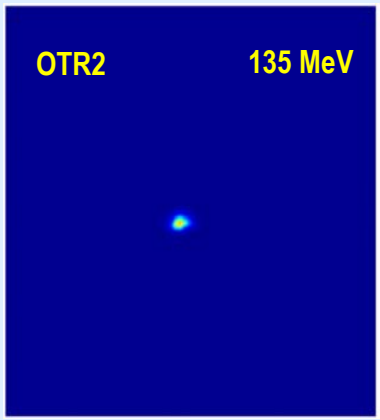

Low Energy RF Deflector on

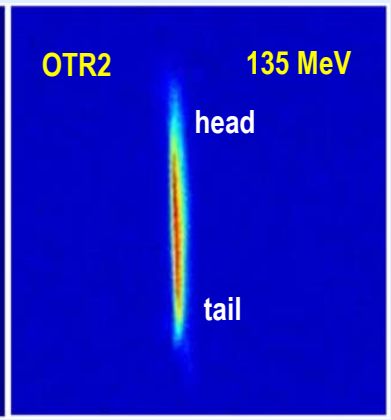

LCLS Bunchlength in front of BC1

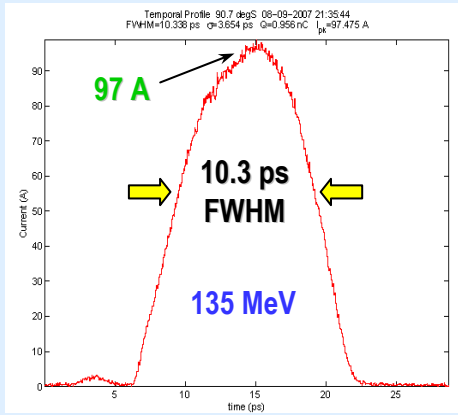

High Energy RF Deflector on

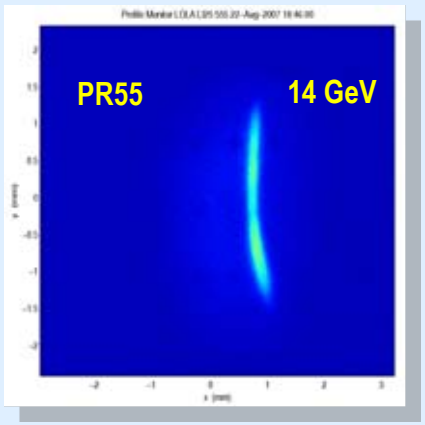

Maximum Compression @ 14 GeV

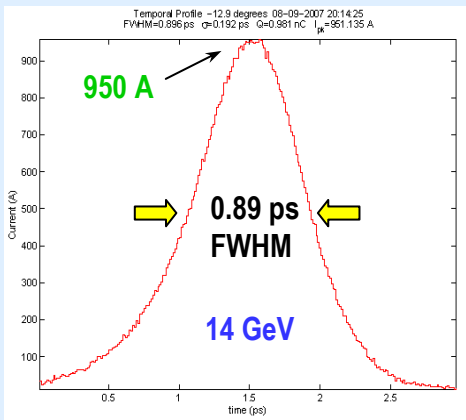

Nominal Compression @ 14 GeV

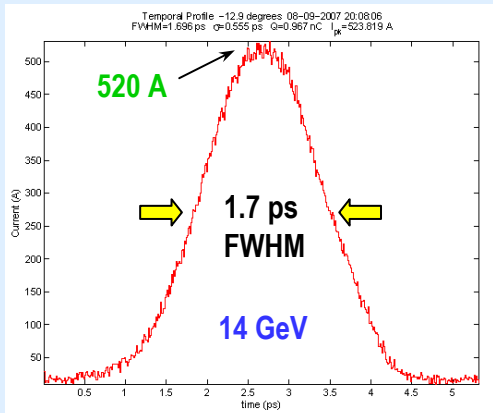

Examples of Bunch Length Measurement with RF Deflector – FLASH

many thanks to Michael Roehrs and the FLASH operations team!
see also: Michael Roehrs, DESY-thesis May 2008
measurements are courtesy of Michael Roehrs, DESY

FLASH Bunchlengths "on crest" Operation

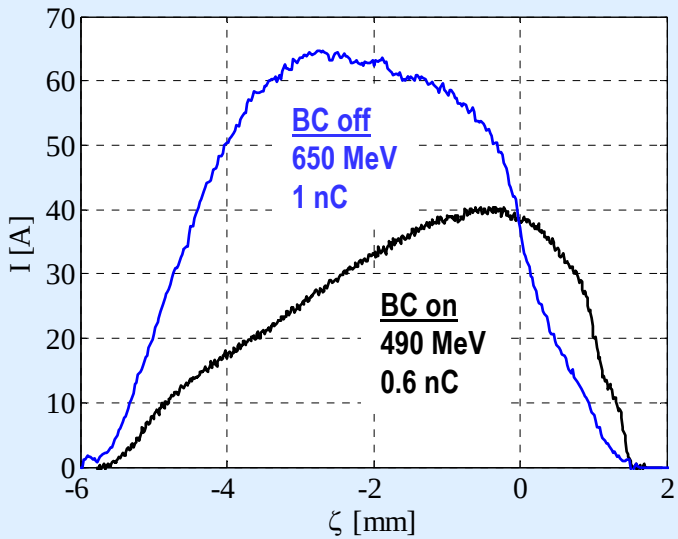

FLASH Bunchlength SASE Operation Modes

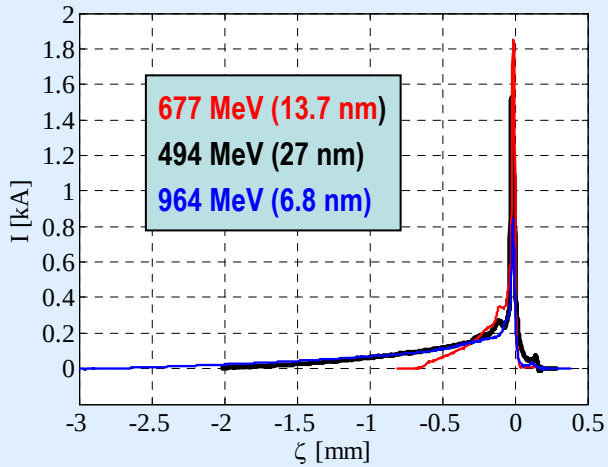

Zoom in FLASH SASE Operation Modes

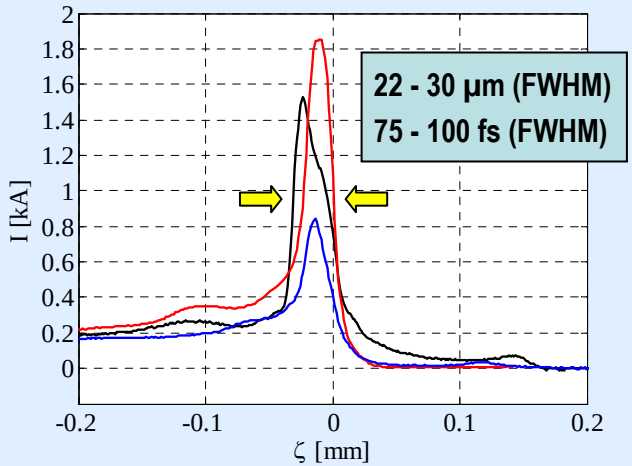

Principle of Time Resolved Energy Spread Measurement with RF Deflector

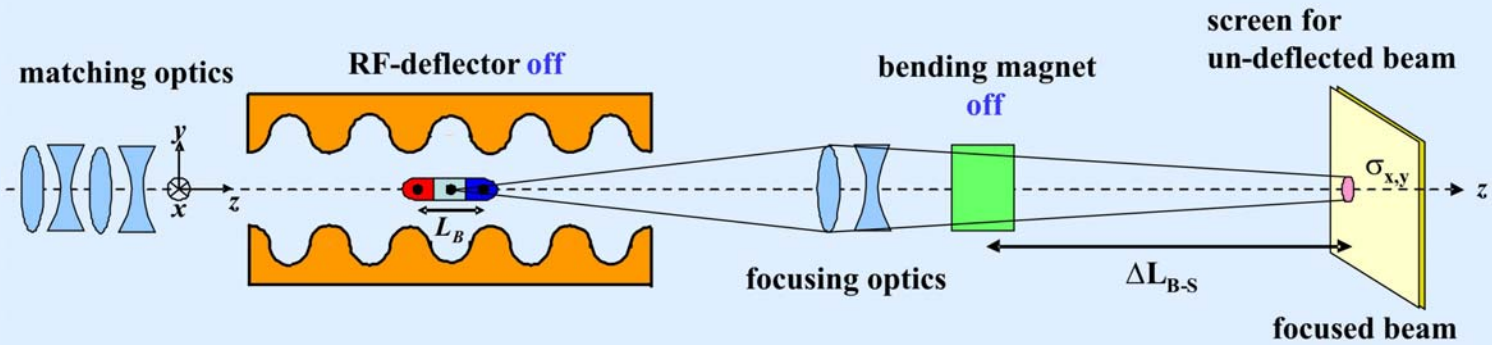

Beam Conditioning for Time Resolved Energy Spread Measurement

with both, RF Deflector and bending magnet off the un-deflected beam should be focused on a screen downstream of the bending magnet to obtain…:

- high temporal resolution (when vertically deflecting)
- good energy resolution (with dispersion dominated beam when switching bending magnet on)

for a finite ε beam, the vertical beam size and thus the temporal resolution limitation is given by:

$$\sigma_{y-screen,\varepsilon} = \sqrt{\frac{\varepsilon_N \cdot \beta_{screen}}{\gamma}}$$

Principle of Time Resolved Energy Spread Measurement with RF Deflector

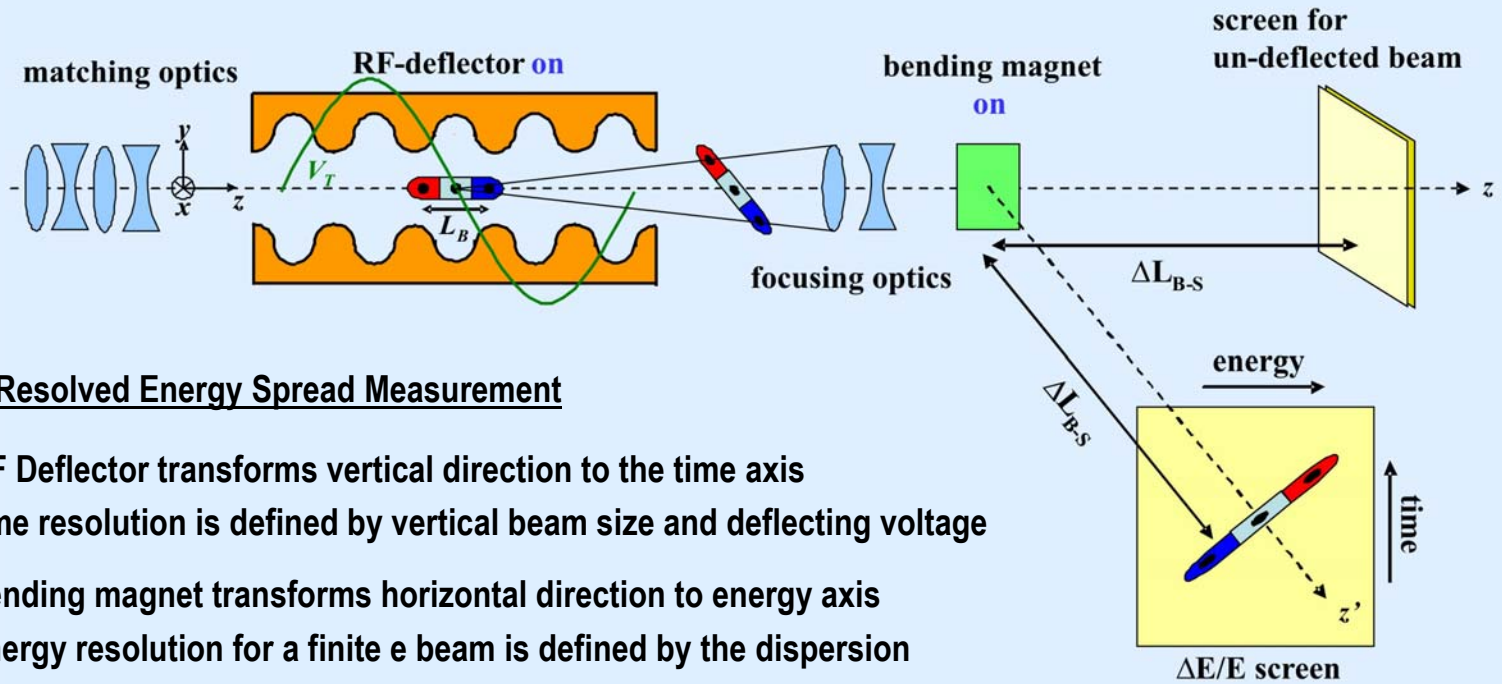

Time Resolved Energy Spread Measurement

- RF Deflector transforms vertical direction to the time axis
- time resolution is defined by vertical beam size and deflecting voltage
- bending magnet transforms horizontal direction to energy axis
- energy resolution for a finite e beam is defined by the dispersion at the screen location:

$$\left.\frac{\Delta E}{E}\right|_{res} = \frac{\sqrt{\varepsilon_x \cdot \beta_{x-screen}}}{D_{screen}}$$

- time slices are usually defined by partition of the image and post processing using image processing SW

Example of Sliced Energy Spread Measurement with RF Deflector – LCLS

many thanks to Paul Emma and the LCLS commissioning team! See also: PR-STAB 11 30703 (2008) about LCLS injector commissioning

Sliced Energy Spread in LCLS Spectrometer @ 135 MeV

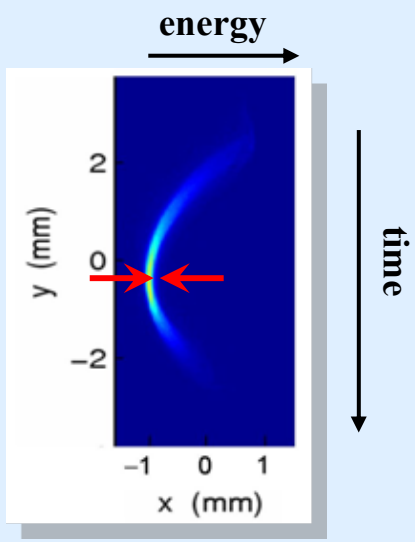

Special lattice configuration (low horizontal β resp. small beam size at screen) in spectrometer allows fine measurement of time-sliced energy spread

$\sigma_E \leq 6$ keV rms (40 μm) at 150 pC bunch charge
(limited to optics resolution of 30-40 μm)

Bunch Compressor

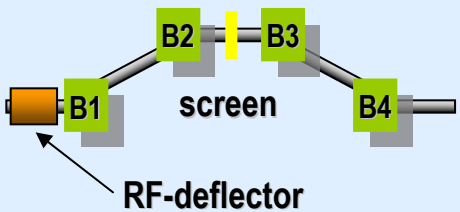

Time Energy Correlation in 1st LCLS Bunch Compressor @ 250 MeV

RF deflector OFF

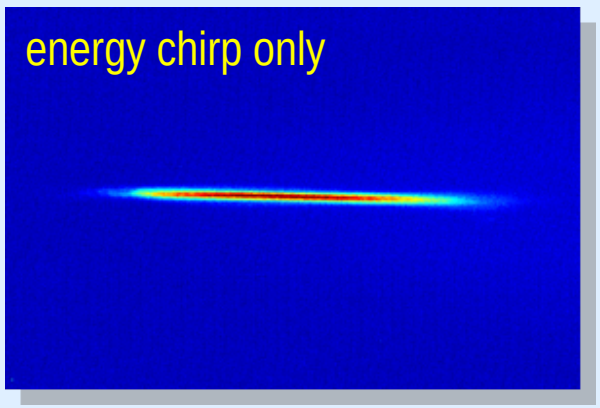

RF deflector ON

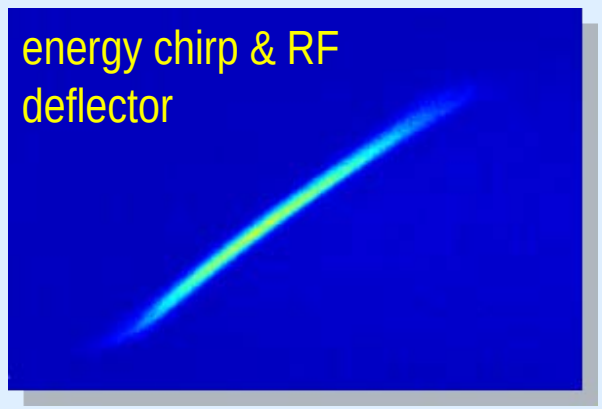

Example of Sliced Energy Spread Measurement with RF Deflector – FLASH

many thanks to Michael Roehrs and the FLASH commissioning team! see also: M. Roehrs, DESY-thesis May 2008, measurements are courtesy of M. Roehrs, DESY

Sliced Energy Distribution @ FLASH

(650 MeV, 1 nC, uncompressed bunches)

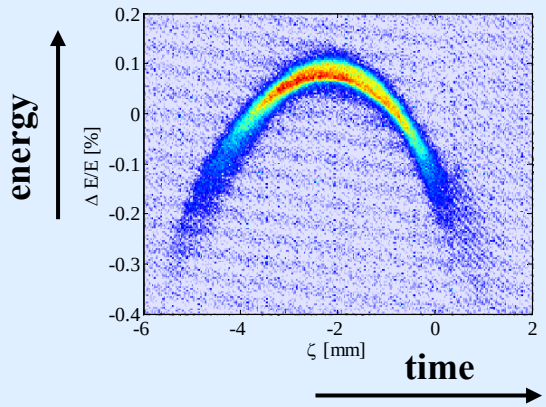

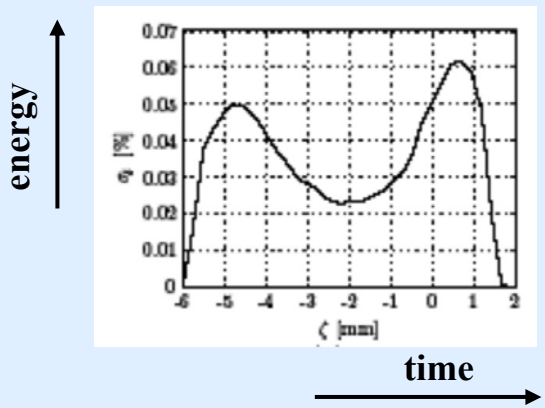

Sliced Energy Distribution @ FLASH

(677 MeV, 0.5 nC, SASE conditions)

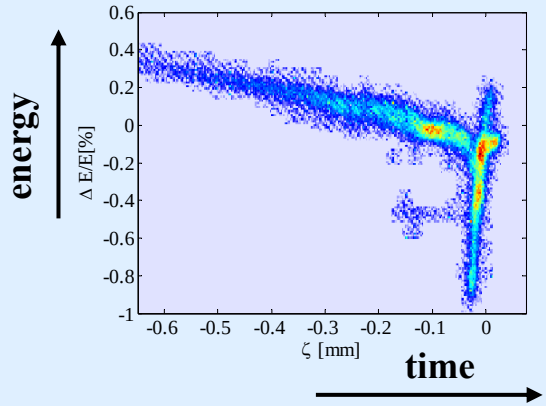

Mean Relative Energy Deviation (50 images)

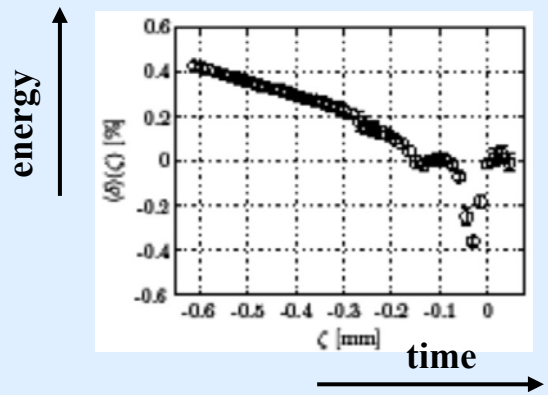

Principle of Time Resolved Emittance Measurement with RF Deflector

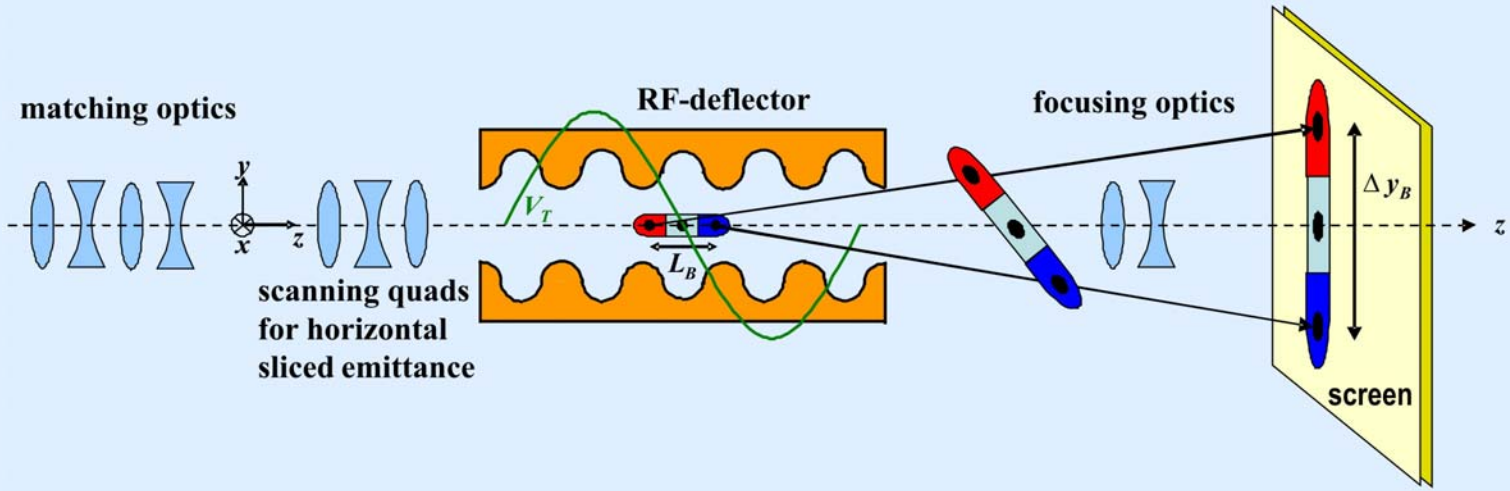

Time Resolved Emitance Measurement ("sliced emittance")

- quadrupole scan in front of or behind RF deflector is used for "sliced emittance" measurement keeping the "shear parameter" of the measurement set-up constant
  - → vertical (deflecting) axis provides time resolution
  - → horizontal axis provides beam emittance
- time slicing of images is obtained by post measurement image processing
- emittance resolution is determined by resolution of optical system
  it should match the co-operation length of the FEL process after final bunch compression stage of an XFEL facility

Example of "Sliced Emittance" Measurement with RF Deflector - LCLS

many thanks to Paul Emma and the LCLS commissioning team! See also: PR-STAB 11 30703 (2008) about LCLS injector commissioning

- bunch has been binned into 12 slices with 1.7 ps slice length – data taken for 135 MeV beam
- horizontal emittance has been calculated for each slice individually – by analyzing quad scan
- "beta mismatch amplitude parameter" ξ describes the difference between measured and design Twiss parameters

Deflected Beam for One Quad Setting

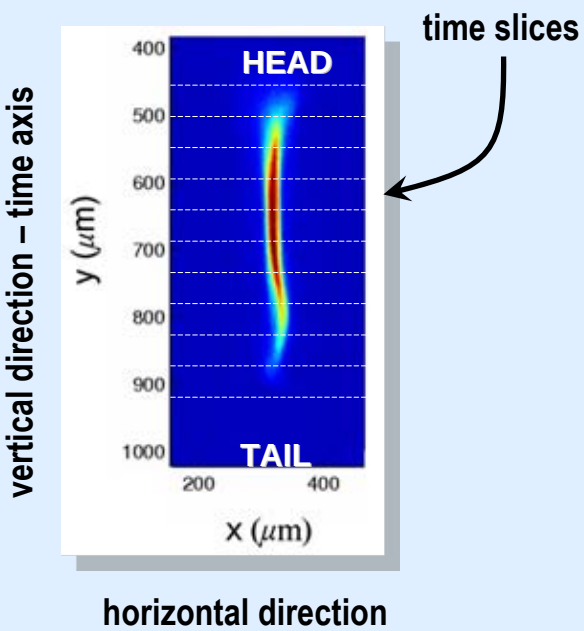

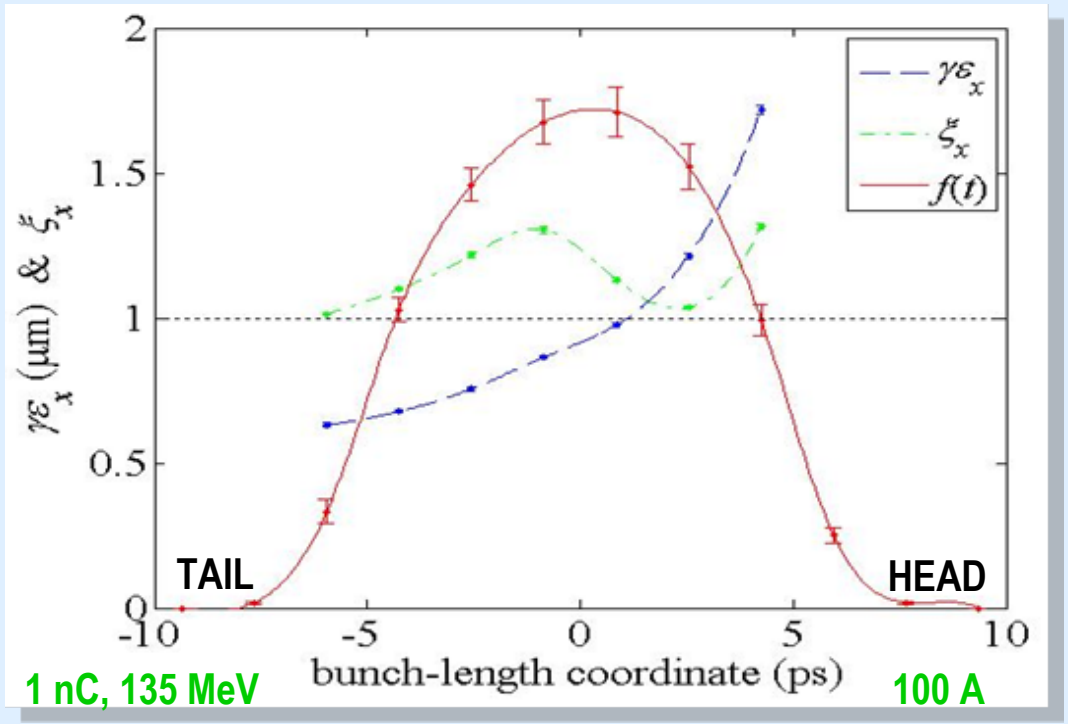

Example of "Sliced Emittance" Measurement with RF Deflector - FLASH

many thanks to Michael Roehrs and the FLASH commissioning team! see also: M. Roehrs, DESY-thesis May 2008, measurements are courtesy of M. Roehrs, DESY

Sliced Emittance Tomography – uncompressed bunch

time slices along bunch | transverse phase space

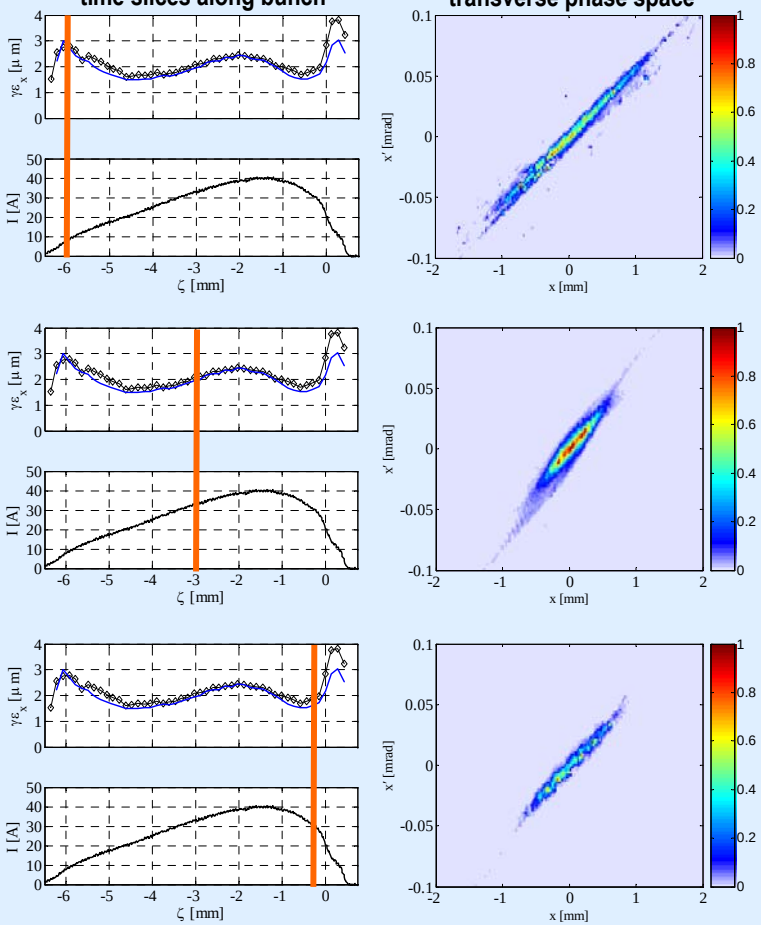

Sliced Emittance Tomography – SASE conditions

time slices along bunch | transverse phase space

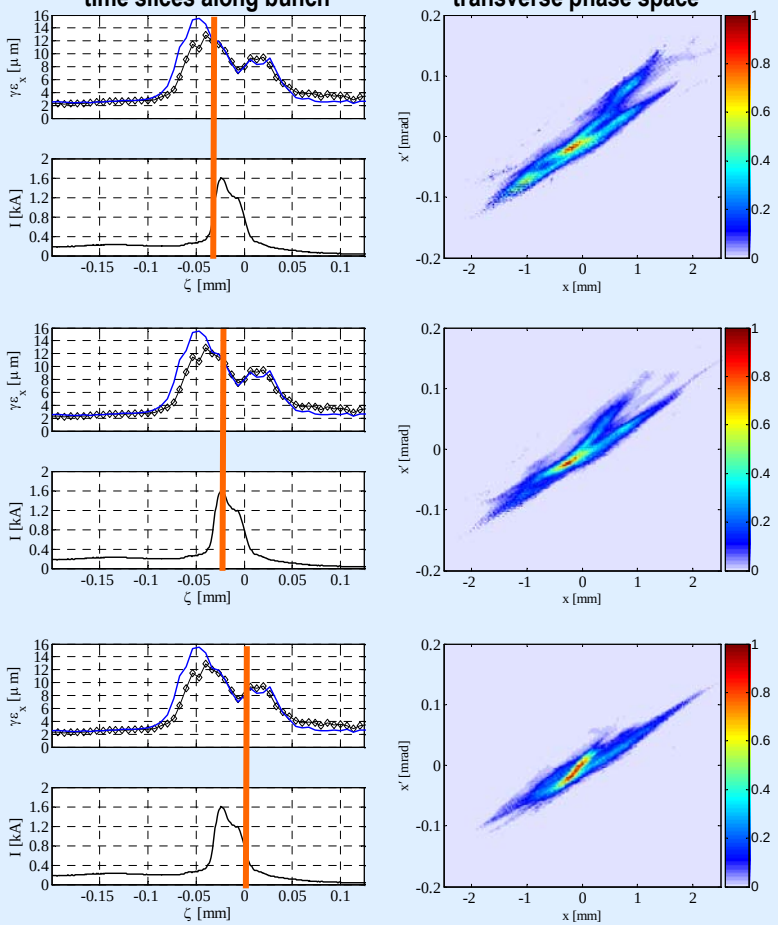

Transverse RF Deflector - Summary

- **transverse RF deflectors are "*fs streak cameras*" for highly relativistic electron beams**

- **traveling wave (LOLA-type) and standing wave (SPARC-type) transverse RF deflectors are very powerful…**

  - bunch length diagnostics
  - "sliced" energy spread diagnostics (complete time resolved longitudinal phase space)
  - "sliced" emittance diagnostics (complete time resolved transverse phase space)

- **transverse RF deflectors can be used for low (SW structures) and high (TW structures) energy particle beams providing excellent (sub – 10 fs) time resolution in single-shot and averaging modes**
  (in averaging mode good RF synchronization is critical !!!)

- **Unfortunately,…**

  RF deflectors are destructive diagnostics and cannot be used "online"

Introduction to Bunch Length Diagnostics using Coherent Radiation

- radiation emitted by relativistic particle beams (in the following: electron beams) contains information about the longitudinal and transverse bunch distribution
- typically Cerenkov radiation (CR), transition and diffraction radiation (TR and DR), synchrotron radiation (SR) edge radiation from bending magnets (ER) and Smith-Purcell radiation (SPR) are used for diagnostics purposes
- at wavelength (much) shorter than the bunch length the radiation is emitted incoherently because each electron emits its radiation independently from the others without a defined phase relation

- coherent enhancement occurs at wavelengths, which are equal to or longer than the bunch length, where fixed phase relations are existing, resulting in the temporal coherence of the radiation
- while the power of the incoherent radiation scales with the number N of particles in a bunch, the coherent radiation increases with the square of the number of particles N^2

Coherent Radiation – The Longitudinal Bunch Form Factor I

formalism adapted from: C. Hirschmugl et al., Phys. Rev. A, vol. 44, number 2 (1991) p. 1316

using classical electrodynamics and the notation of Jackson, the radiation emitted by a single electron in the far field ($R >> r$), into a solid angle $d\Omega$ in a frequency range $d\omega$ is given by:

$$\frac{d^2 I}{d\omega\, d\Omega} = \frac{e^2 \omega^2}{4\pi^2 c}\left|\int_{-\infty}^{\infty} \hat{n}\times\left(\hat{n}\times\beta\right) e^{i\omega\left[t-\hat{n}\cdot r(t)/c\right]} dt\right|^2$$

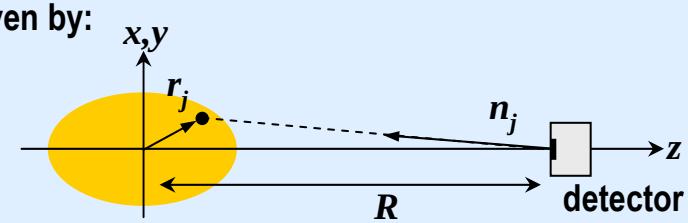

→ for a bunch with N particles:

$$\frac{d^2 I}{d\omega\, d\Omega} = \frac{e^2 \omega^2}{4\pi^2 c}\left|\int_{-\infty}^{\infty} \sum_{j=1}^{N} \hat{n}\times\left(\hat{n}\times\beta_j\right) e^{i\omega\left[t-\hat{n}\cdot r_j(t)/c\right]} dt\right|^2$$

with β_j as the ratio of the jth particle to the velocity of light (v_j / c) and r_j the position of the jth particle in the bunch

assuming β as the same velocity for all particles in the bunch and $r(t)$ as their persistent position in relation to the center of mass of the bunch, the above relation can be rewritten to:

$$\frac{d^2 I}{d\omega\, d\Omega} = \frac{e^2 \omega^2}{4\pi^2 c}\left|\sum_{j=1}^{N} e^{i\omega r_j/\beta c}\right|^2 \left|\int_{-\infty}^{\infty} \hat{n}\times\left(\hat{n}\times\beta\right) e^{i\omega\left[t-\hat{n}\cdot r(t)/c\right]} dt\right|^2 \qquad \text{and with } \beta = 1\ldots: \qquad T(\omega) = \left|\sum_{j=1}^{N} e^{i\omega r_j / c}\right|^2$$

the time dependent terms have been separated from the summation term and remain in the integral, which represents the intensity radiated by single (particle) electron

Coherent Radiation – The Longitudinal Bunch Form Factor II

formalism adapted from: C. Hirschmugl et al., Phys. Rev. A, vol. 44, number 2 (1991) p. 1316

$$T(\omega) = \left| \sum_{j=1}^{N} e^{i\omega r_j / c} \right|^2 = \sum_{j=1}^{N} e^{i\omega r_j / c} \sum_{k=1}^{N} e^{-i\omega r_k / c} = \sum_{j=1 (j=k)}^{N} e^{i\omega (r_j - r_k)/c} + \sum_{j,k=1 (j \neq k)}^{N} e^{i\omega (r_j - r_k)/c}$$

which in turn becomes unity for $j = k$ and turns into…: $N + \sum_{j,k=1 (j \neq k)}^{N} e^{i\omega (r_j - r_k)/c}$

This equation can be rewritten as…:

$$T(\omega) = N + N(N-1) F(\omega) \quad \textit{with} \quad F(\omega) = \frac{1}{N(N-1)} \sum_{j,k=1 (j \neq k)}^{N} e^{i\omega (r_j - r_k)/c}$$

and the total radiated power by an electron bunch with N particles results in…:

$$\frac{d^2 I}{d\omega \, d\Omega} = \left[N + N(N-1) F(\omega) \right] P(\omega)$$

where $P(\omega)$ is the power radiated by a single electron and $F(\omega)$ describes the coherence of the emitted radiation

$F(\omega) = 0$	represents the incoherent limit with the total power ~ the number of particles N
$F(\omega) = 1$	represents the coherent limit with the total power ~ the square of the number of particles N^2

Coherent Radiation – The Longitudinal Bunch Form Factor III

formalism adapted from: C. Hirschmugl et al., Phys. Rev. A, vol. 44, number 2 (1991) p. 1316

In particle accelerators, it is usually justified to assume:

- a continuous particle distribution $S(r)$
- with a large number N of particles in a bunch (typically 10^7 – 10^{12})

This allows the expression of $$F(\omega) = \lim_{N\to\infty} \frac{1}{N^2} \sum_{j,k=1(j\neq k)}^{N} e^{i\omega(r_j - r_k)/c}$$

by the *Fourier Integral of the charge distribution function*

$$F(\omega) = \left| \int e^{i\omega r/c} S(r) dr \right|^2$$

by assuming a circular transverse beam distribution in the far field ($R >> r_{bunch}$), the formfactor $F(\omega)$ depends only on the longitudinal charge distribution:

$$F(\omega) = \left| \int e^{i\omega z/c} S(z) dz \right|^2$$

Coherent Radiation – Bunch Compression & Longitudinal Bunch Form Factor

Magnetic Bunch Compression (Schematic)

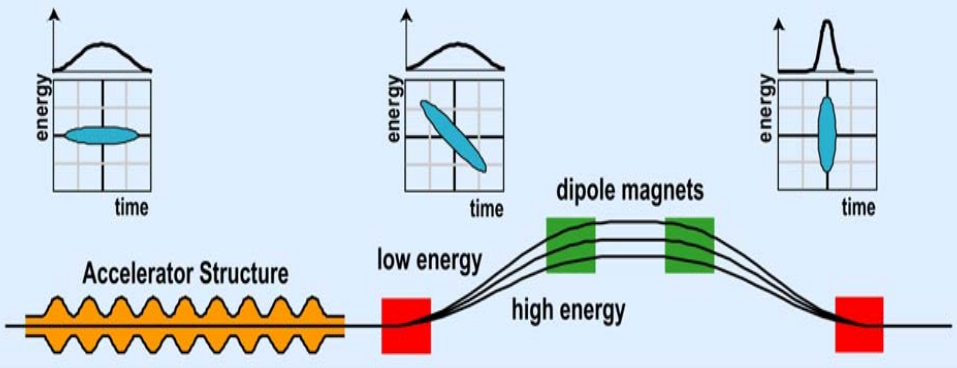

Longitudinal Phase Space at FLASH

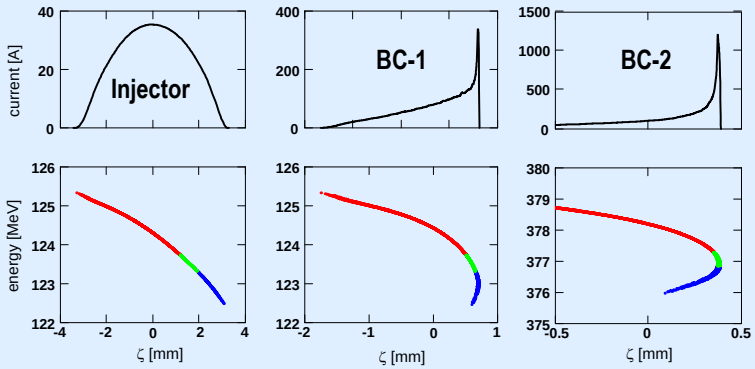

courtesy of M. Dohlus (DESY)

LINAC…:

example taken from
Jan Menzel (PhD) :
FLASH bunches

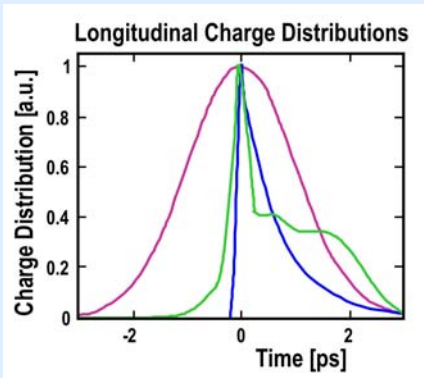

$$\left| \int e^{i\omega z/c} S(z) dz \right|^2$$

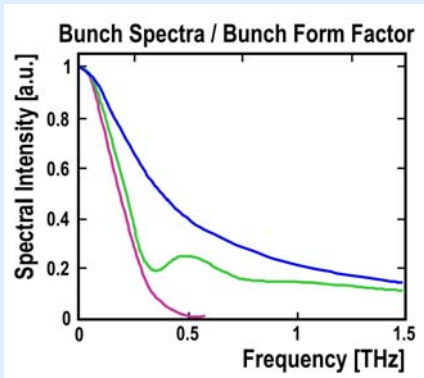

bunch length meas. with coherent radiation typical units:

1 ps	~ 1 THz ~ 300 μm ~ 33 cm^{-1} ~ 4.1 meV ~ 47.6 K
100 fs	~ 10 THz ~ 30 μm ~ 333 cm-1 ~ 41 meV ~ 476 °K

Coherent Radiation – Bunch Slicing & Longitudinal Bunch Form Factor

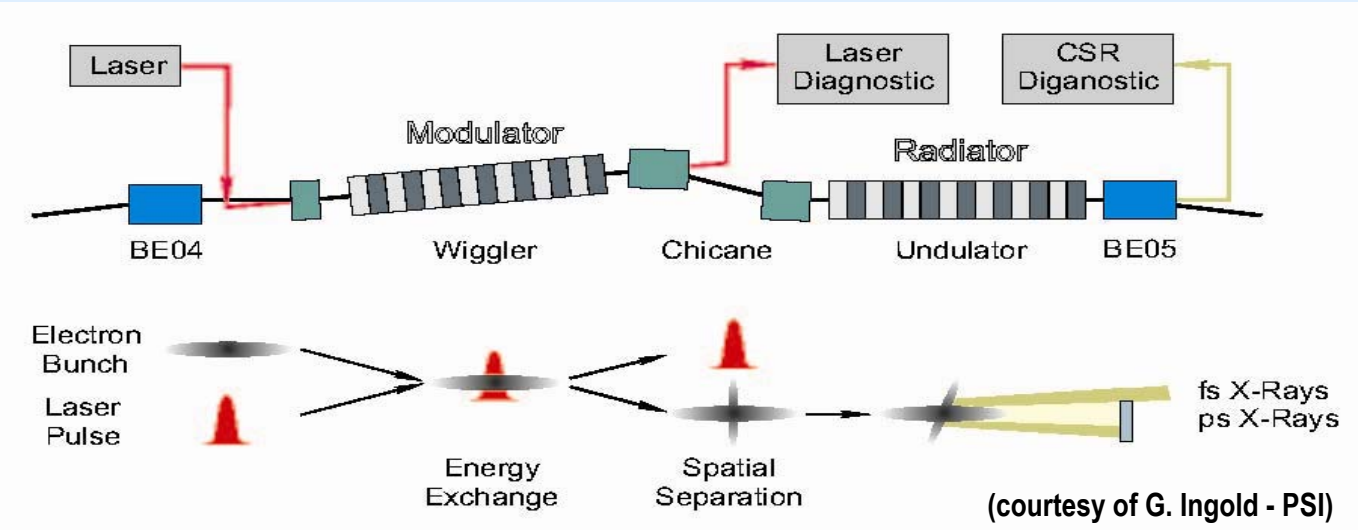

(courtesy of G. Ingold - PSI)

FEMTO-Bunch Slicing in SLS Storage Ring…:

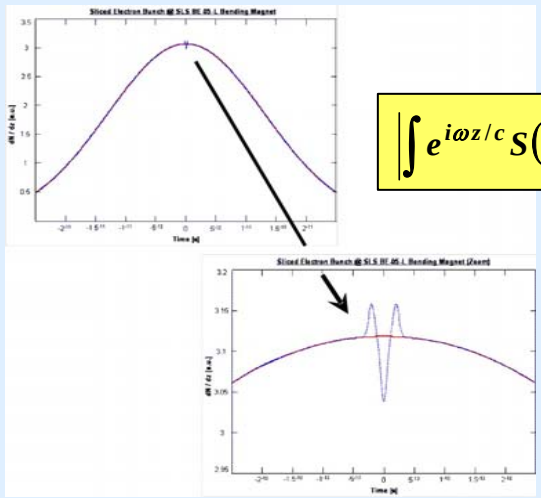

$$\left|\int e^{i\omega z/c} S(z) dz\right|^2$$

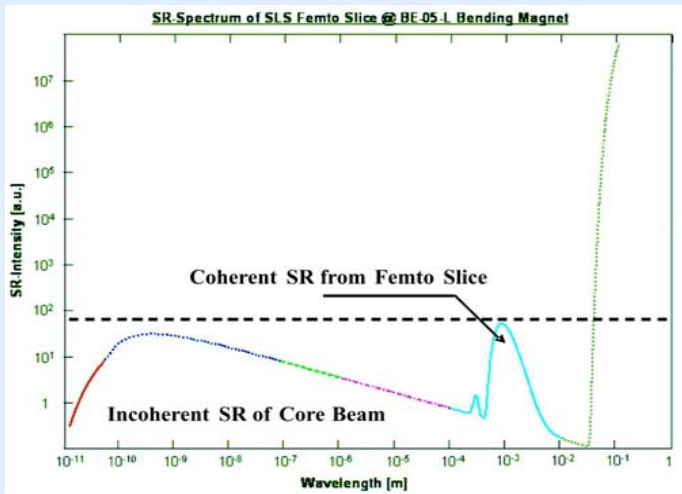

Coherent Radiation – SLS FEMTO Bunch Slicing Experiment

SLS FEMTO Source: Hard X-Rays

(courtesy of G. Ingold – PSI)

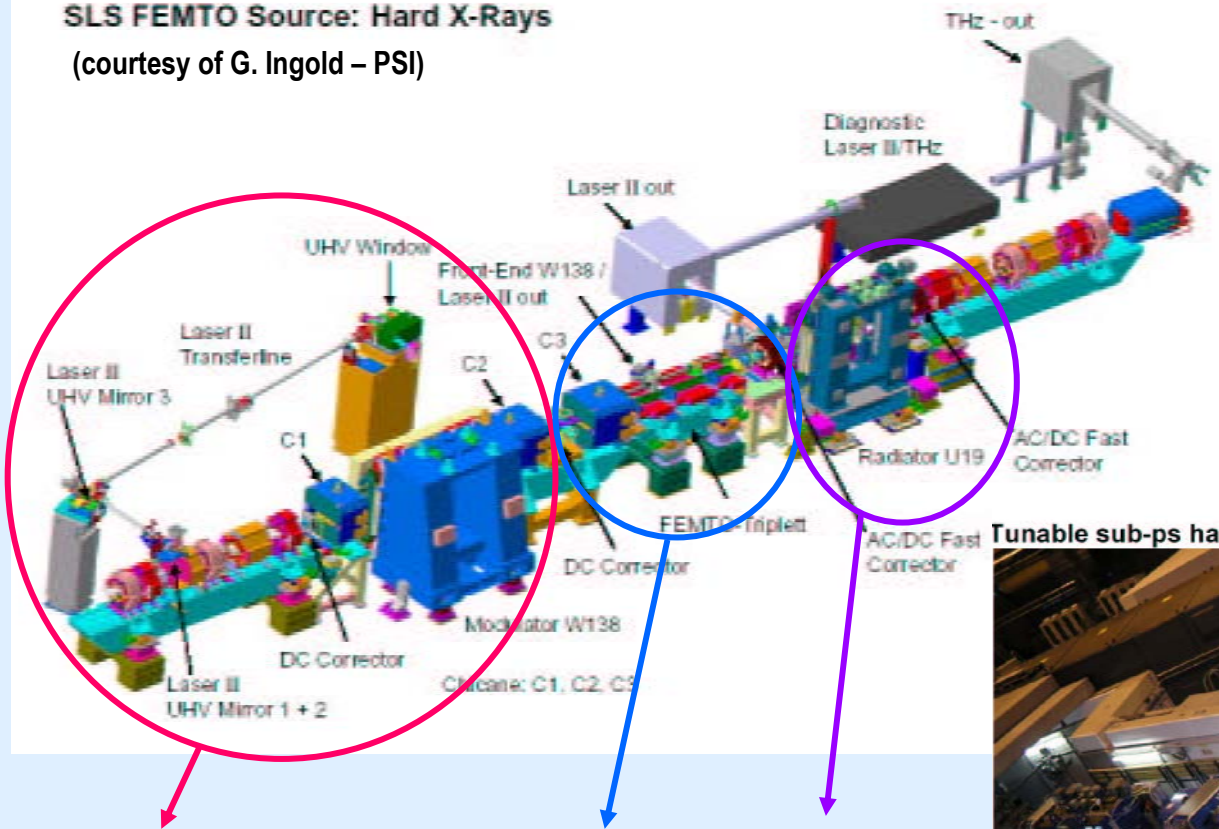

Tunable sub-ps hard X-ray (3-18 keV) source

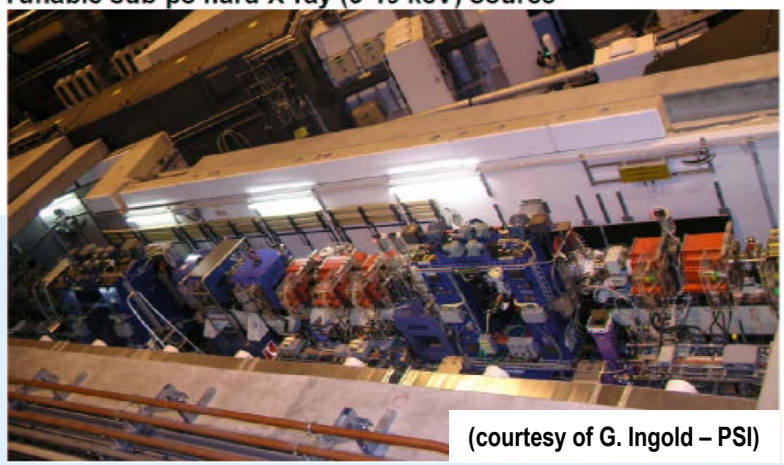

(courtesy of G. Ingold – PSI)

Electron/Laser Interaction
Modulator
(Wiggler)

Pulse Separation
Angular Dispersion
(Chicane Magnets)

Sub-ps X-Rays
Radiator
(Bend / Undulator)

Coherent Radiation – Emission Spectrum

for sub-ps (electron) bunches, the wavelength range of coherent emission is typically in the sub-mm & THz-regime

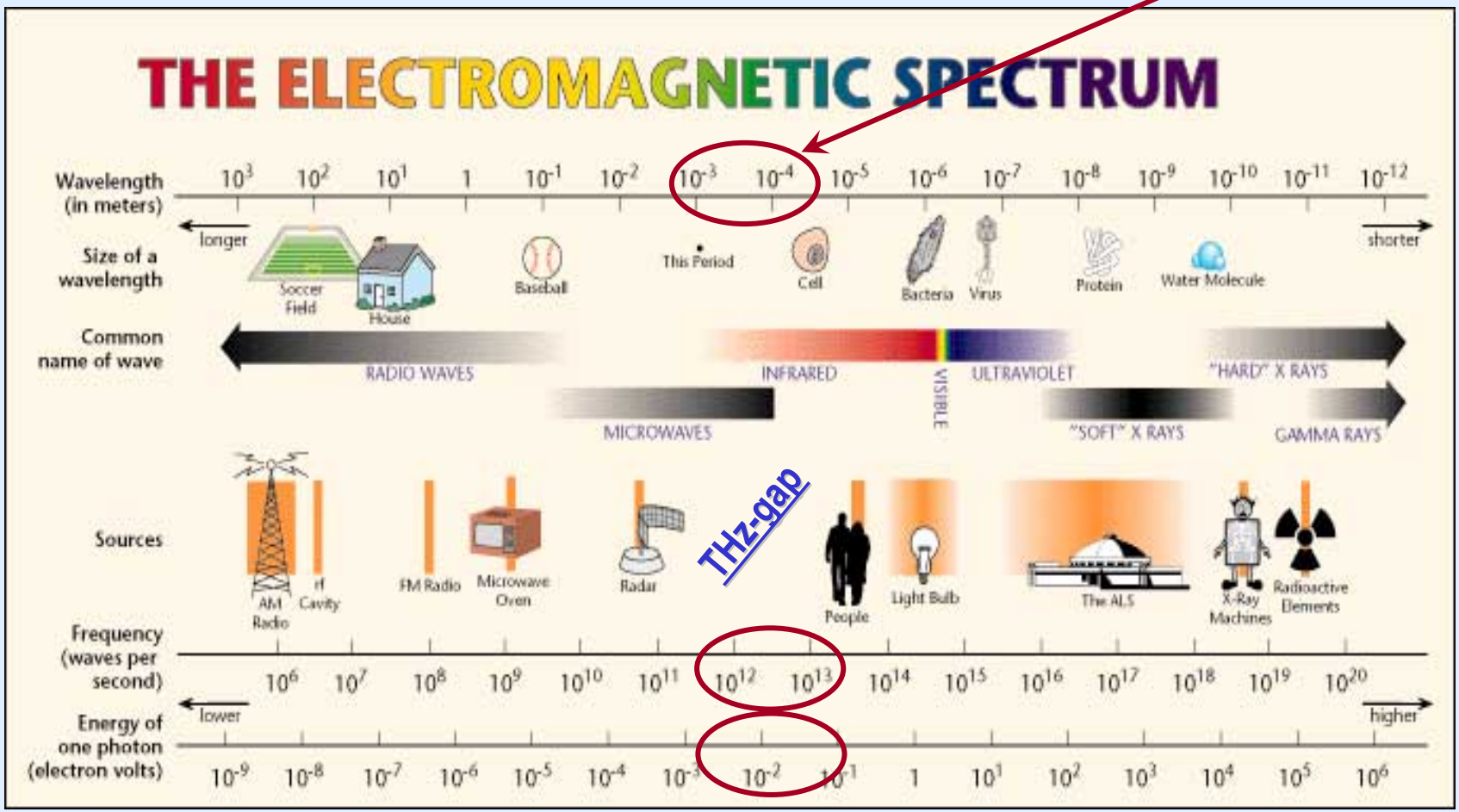

Coherent Radiation – Peculiarities of Sub-mm (THz) Wavelengths

- opening angles of coherent radiation (CSR, CER, CTR and CDR…) emitted from highly relativistic particle beams are much wider than the usual 1/γ approximation

Opening Angles of Coherent TR (vertical polarization) in the Sub-mm (THz) Regime (Theory & Measurement)

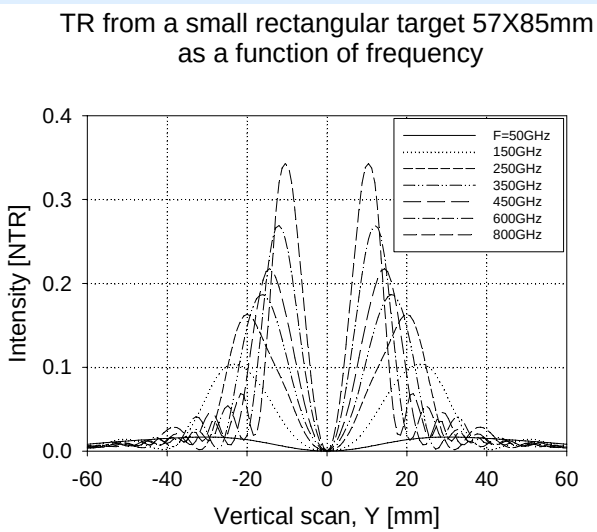

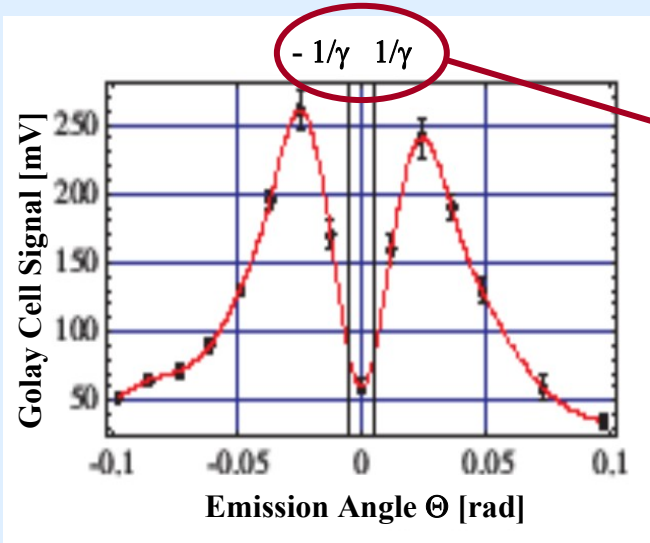

Ginzburg-Frank relation for the emission angle of TR in the visible and IR wavelength regime

- *Gauss Optics* needs to be applied for design of THz beam transport systems
  - → large apertures of so called quasi optical elements are required
  - → first surface metal mirrors (typically gold coated) are used for beam transport (plane mirrors) and focusing (paraboloids, toroids etc…)

Coherent Radiation – Peculiarities of Sub-mm (THz) Wavelengths

Transmission of Typical (UH) Vacuum Window Materials

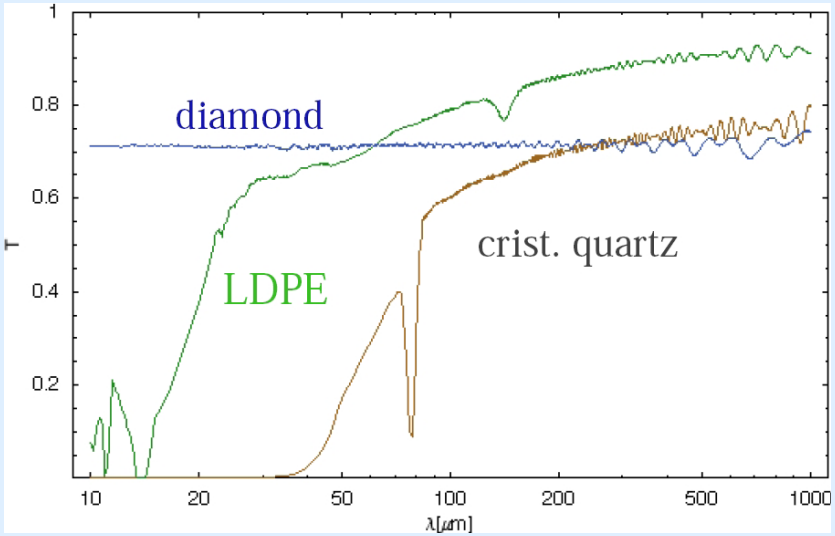

Water Absorption as a Function of Air Pressure

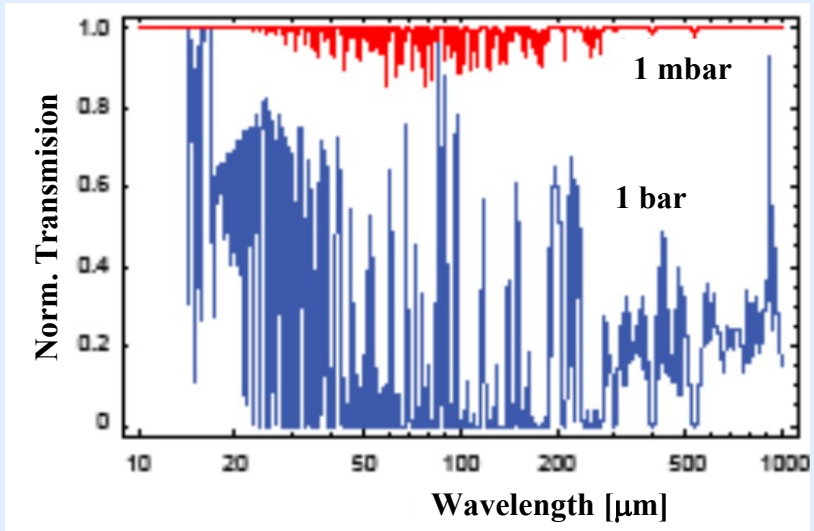

Optical set-ups and beam transport lines have to be well designed for sub-mm (THz) radiation

- → **beam transport should be done with large aperture mirror optics**
- → **special materials for UHV windows (Diamond for fs bunches, Crystal Quartz well suitable for ps-pulses)**
- → **optical set-ups should be in vacuum (some mbar) or flooded with Nitrogen**

Coherent Radiation – Example of SLS FEMTO THz Beam Transport Line

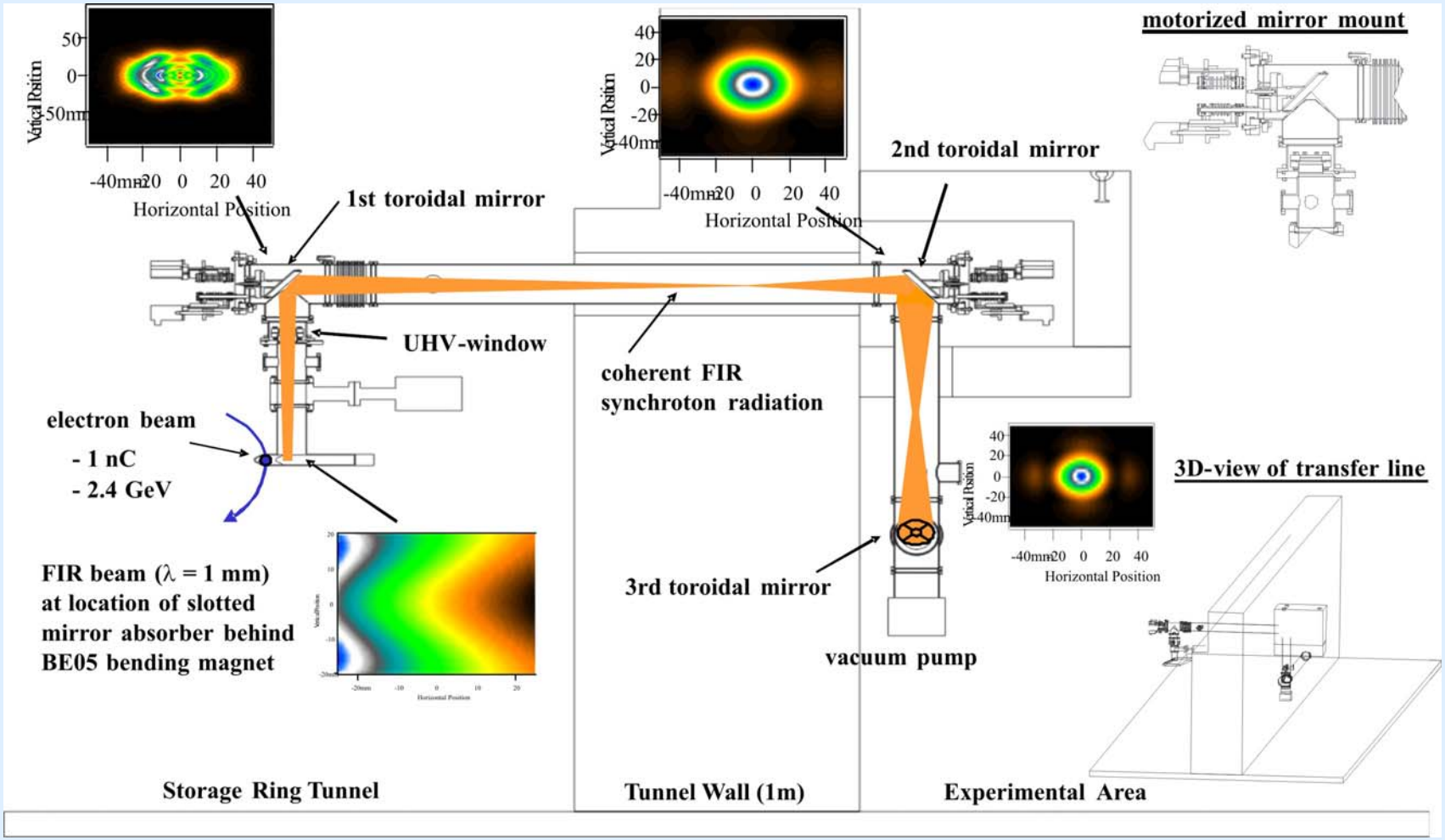

Coherent Radiation – Detector Systems in the THz Regime

He- and N-cooled bolometers (InSb, Si, GeGa, Nb…)

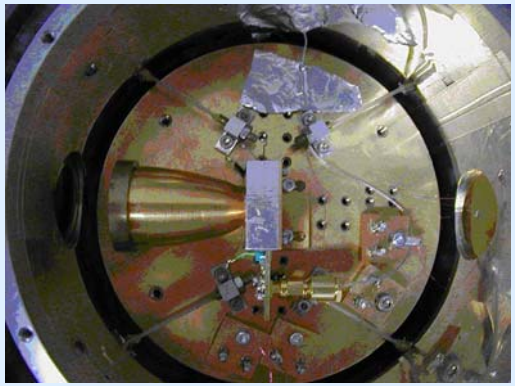

Spectral response: ~ 5 mm to < 50 μm
Optical N.E.P: ~ 1.5 · 10^{-12} W·Hz $^{-1/2}$
Dynamic Range: pW to μW
Opt. Responsitivity: 15 kV / Watt
Detector BW: ~ 1 MHz
Operating Temp.: < 4.2 °K
Price: ~ 20 – 30 k£

Golay Cell Detectors

Spectral response: ~ 5 mm to visible
Optical N.E.P: ~ 1 · 10^{-10} W·Hz $^{-1/2}$
Dynamic Range: pW to μW
Opt. Responsitivity: 100 kV / Watt
Detector BW: ~ 15 Hz
Operating Temp.: 300 °K
Price: ~ 8 k£

Other useful FIR (THz) detectors are e.g.: Pyro-Electric Detectors ($LiTaO_3$) and DTGS Detectors

Spectral response: ~ 5 mm to < 5 μm
Optical N.E.P: ~ 2 · 10^{-9} W·Hz $^{-1/2}$
Dynamic Range: nW to mW
Opt. Responsitivity: 10 kV / Watt
Detector BW: ~ 15 Hz
Operating Temp.: 300 °K
Price: ~ 2 – 5 k€

Coherent Radiation – Transfer Function $G(\omega)$ of Measurement System

Transfer Function $G(\omega)$ accounts for wavelength dependent properties of all components in the THz measurement system (here: SLS FEMTO bunch slicing diagnostic)

Crystal Quartz and LDPE Windows

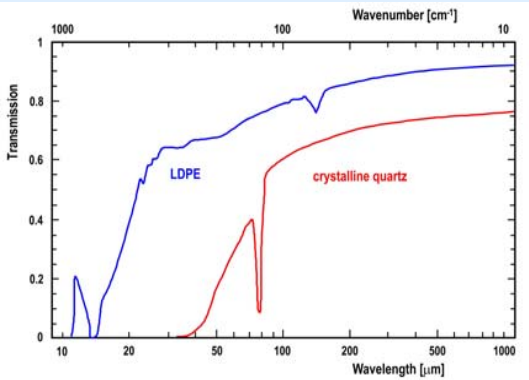

Diffraction through THz Transfer Line

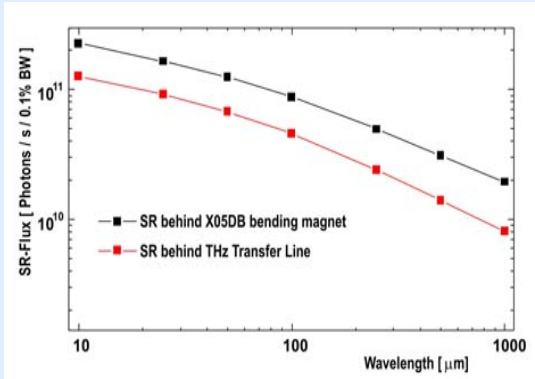

Water Absorption through 0.5 m (MPI)

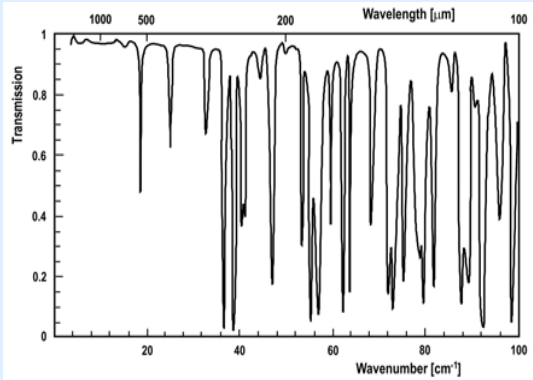

Liquid He-cooled InSb Bolometer

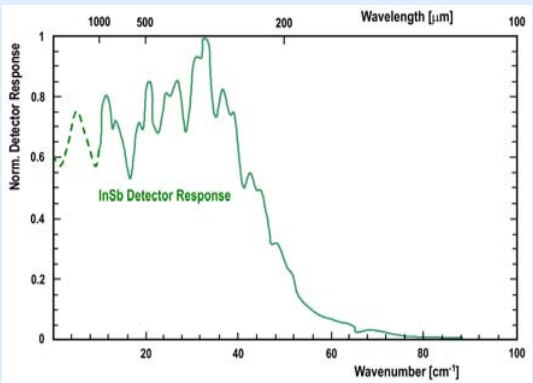

$$G(\omega) = \prod_i G_i(\omega)$$

Transfer Function of FEMTO Slicing Diagnostics Line

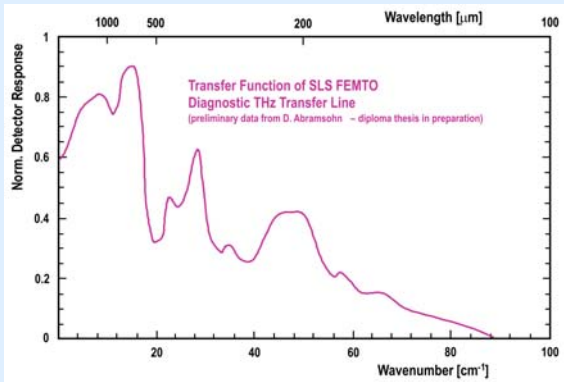

Measurements with Coherent Radiation: LCLS Bunching Monitor

many thanks to J. Frisch & H. Loos and the LCLS commissioning team! See also: PR-STAB 11 30703 (2008) about LCLS injector commissioning

Coherent Edge Radiation from 4th Bend of BC-1

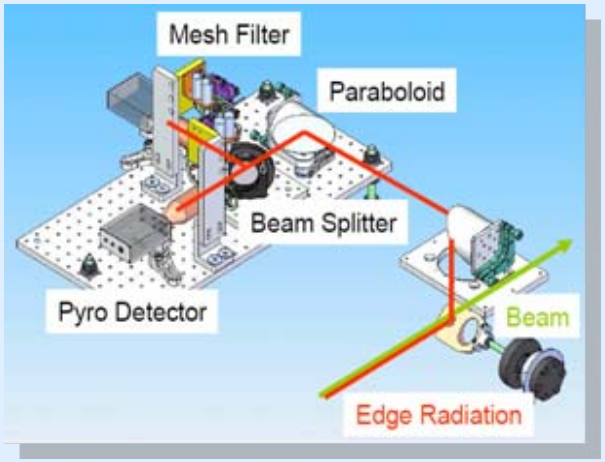

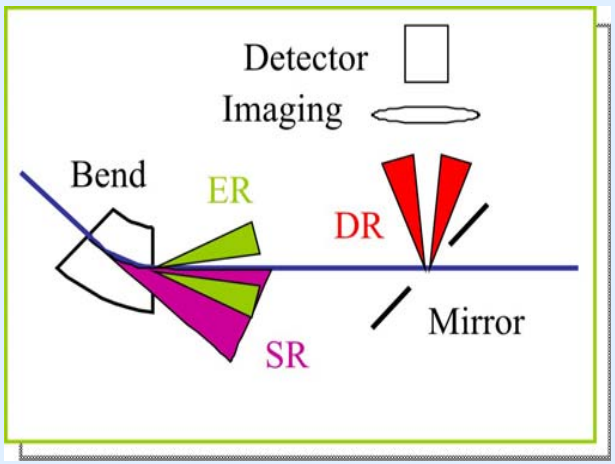

Signals from Pyro-Electric Detectors for Different RF Phases

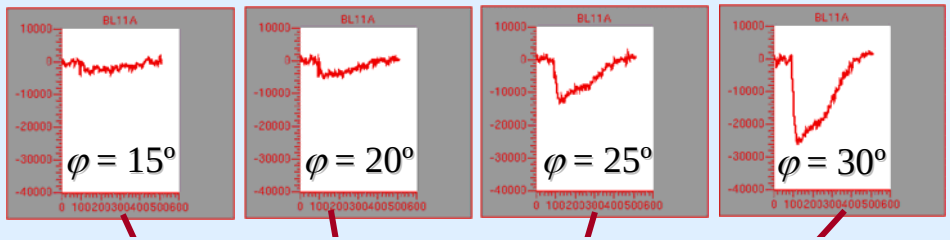

RF Phase Scan behind BC-1 using CER from 4th Bending Magnet

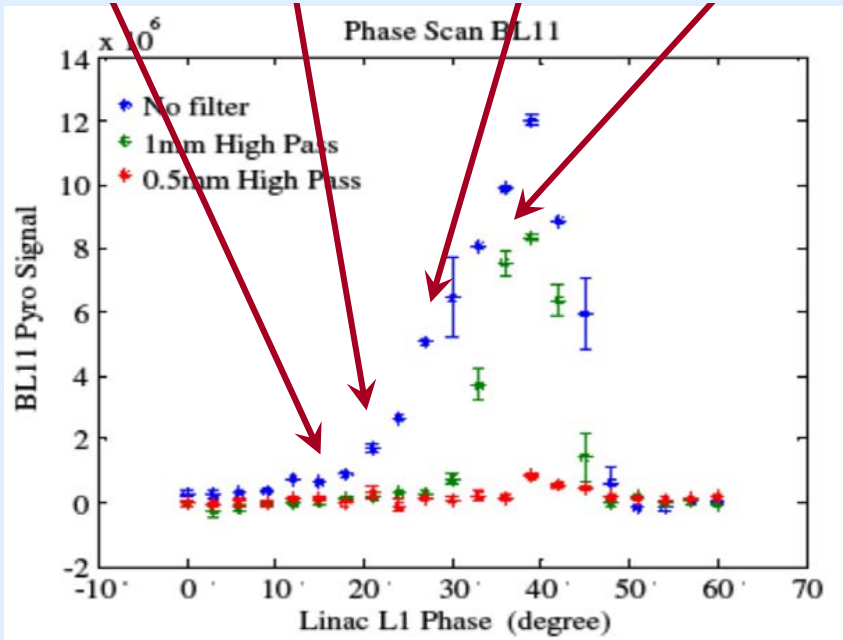

Measurements with Coherent Radiation – Martin-Puplett Interferometer

Schematic of MPI for Coherent Transition Radiation

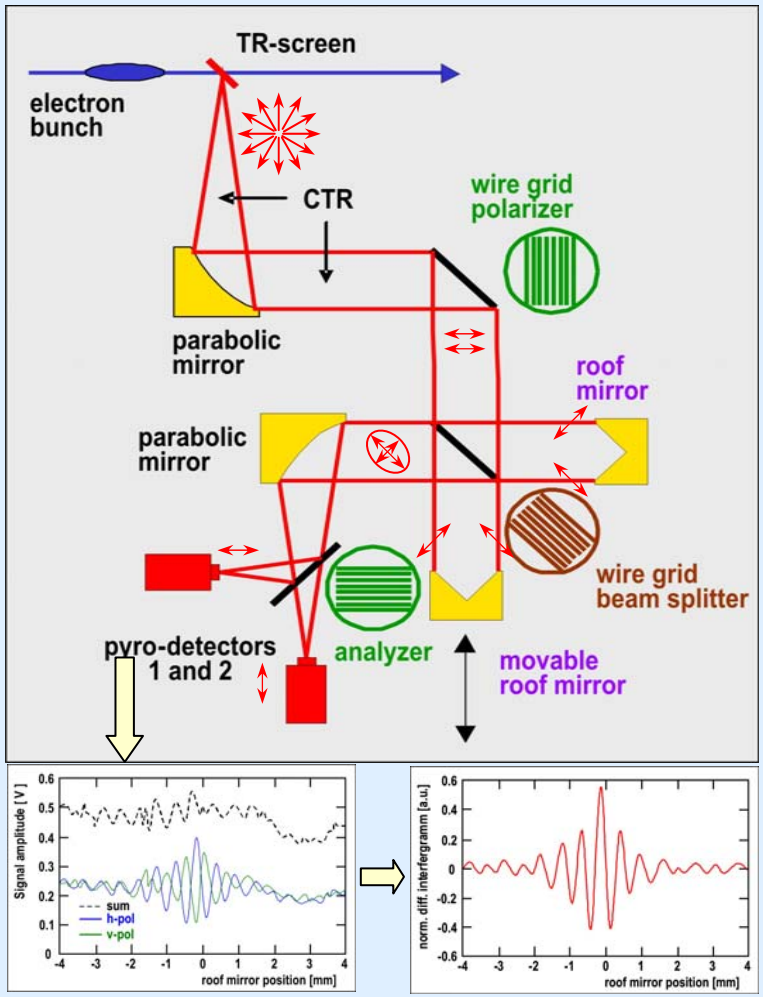

interferometer scans are courtesy of Lars Fröhlich, DESY

MPI Operating Principle…:

- the MPI works like the well known *Michelson Interferometer* but takes advantage of the polarization of CTR, CSR…
- *radially* polarized CTR is transferred into *linearly* polarized light at the wire grid polarizer (in reflection or transmission)
- at the wire grid beam splitter (oriented at 45° in projection / 35.3° in the horiz. plane) half of the linearly polarized light is reflected and half is transmitted
- the roof mirrors in the interferometer arms flip the polarization state of the radiation so that the previously reflected beam is now transmitted at the wire gird beam splitter and vice versa
- recombination of the two linearly polarized light waves with perpendicular polarization states leads – in case of different path lengths in the interferometer arms – to elliptically polarized light
- the analyzer grid separates again the horizontal and vertical polarization states of the radiation
- the wavelength dependent phase differences in the MPI arms lead to different intensities of the two polarization states at the detectors

Measurements with Coherent Radiation – Martin-Puplett Interferometer

Martin-Puplett Interferometer installed behind FLASH Synchrotron Radiation Beamline

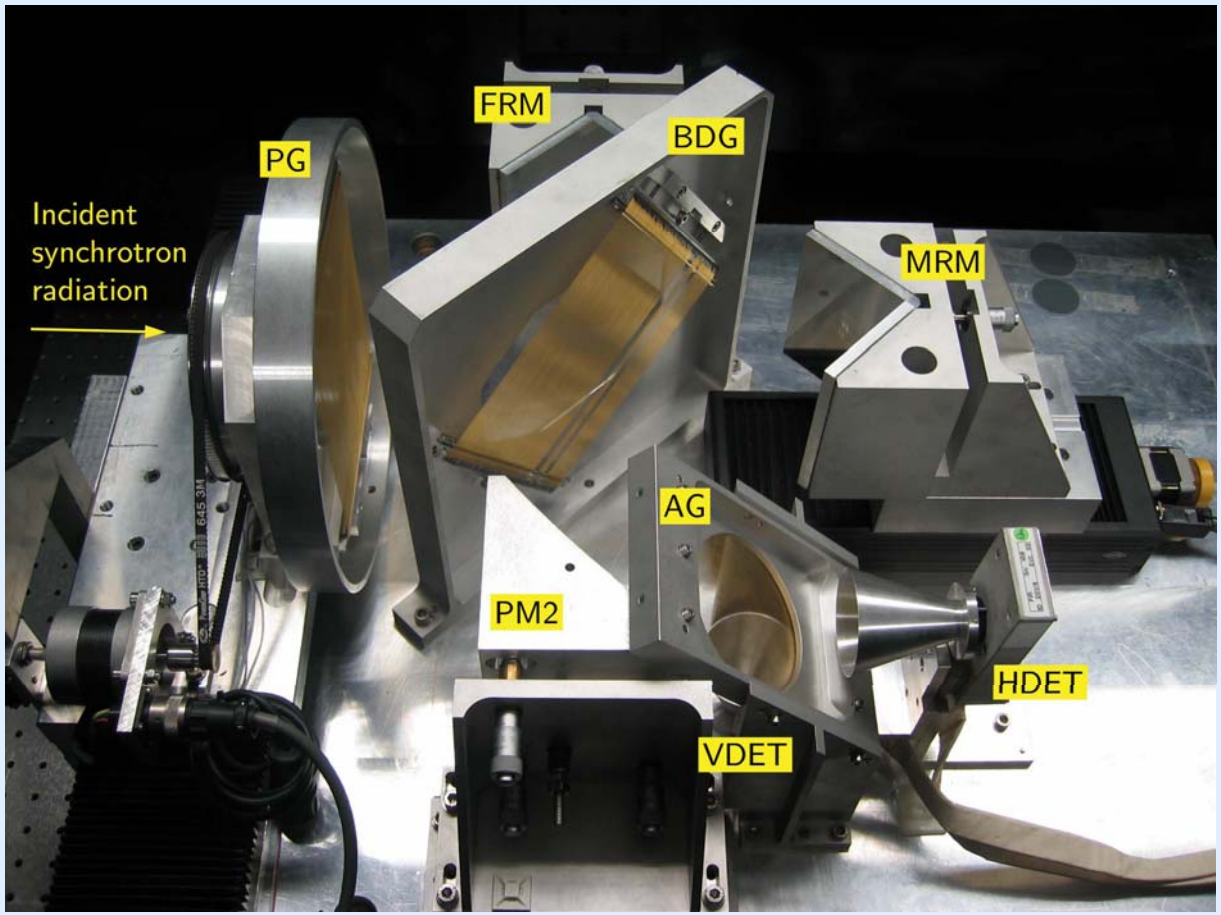

courtesy of Lars Fröhlich, DESY

- **PG** - polarizing grid
- **BDG** - beam splitter grid
- **FRM** - fixed roof mirror
- **MRM** - movable roof mirror
- **PM2** - parabolic mirror
- **AG** - analyzing grid
- **VDET** - pyro-detector for vertical polarization
- **HDET** - pyro-detector for horiz. polarization

Measurements with Coherent Radiation – Fourier Spectroscopy I

- incoming *E-M wave* with horizontal polarization (*behind polarizer*)…:

$$E_{in}(\omega,t) = E_{in}(\omega)\cdot\sin(\omega t)\vec{e}_h$$

- *E-M wave behind wire grid beam splitter* (45°)…:

$$E_{1,2}(\omega,t) = \frac{E_{in}(\omega)}{2}\cdot\sin(\omega t)\left(\vec{e}_h \pm \vec{e}_v\right)$$

- from *roof mirrors back reflected E-M wave* (90° pol. rotated)…:

$$E_{1,2}(\omega,t) = \frac{E_{in}(\omega)}{2}\cdot\sin\left(\omega\left(t+\Delta t_{1,2}\right)\right)\left(\vec{e}_h \mp \vec{e}_v\right)$$

- *interfering the E-M waves behind beam splitter*…:

$$E_{out}(\omega,t) = E_1(\omega,t) + E_2(\omega,t)$$

- the *mean intensity at the detectors* (slow compared to ω) results to…:

$$I_{1,2}(\omega) = \overline{\left(E_{out}(\omega,t)\cdot\vec{e}_{h,v}\right)^2}$$

- using $\tau = (\Delta t_1 - \Delta t_2)$ and $I_{in}(\omega) = E_{in}(\omega)^2/2$, the *intensities at the detectors* can be expressed by…:

$$I_1(\omega) = I_{in}(\omega)\cos^2\left(\frac{\omega\tau}{2}\right)$$

$$I_2(\omega) = I_{in}(\omega)\sin^2\left(\frac{\omega\tau}{2}\right)$$

… integration over all frequencies ω leads to interferograms at both detectors:

$$I_{1,2}(\tau) = \int_0^\infty d\omega \frac{I_{in}(\omega)}{2}\cdot\left(1 \pm \cos(\omega\tau)\right)$$

Measurements with Coherent Radiation – Fourier Spectroscopy II

• the MPI difference interferograms result in a *Cosine-Transformation* of the incoming radiation spectrum $I_{in}(\omega)$…:

$$I_{1,2}(\tau) = \int_0^\infty d\omega \frac{I_{in}(\omega)}{2} \cdot (1 \pm \cos(\omega\tau))$$

• the intensity of coherent radiation (CTR, CDR, CSR…) in case of bunch length measurements (N >> 1) results in…:

$$I_{in}(\omega) = N^2 I_{sp}(\omega) |F(\omega)|^2 \cdot \prod_i G_i(\omega)$$

…where $I_{sp}(\omega)$ is the *spectral intensity from a single particle in a bunch*
$F(\omega)$ is the *bunch form factor*
$G_i(\omega)$ is the *frequency dependent transfer function from the bunch to the detector*

• intensity fluctuations are eliminated by using interferograms from both detectors for data analyses

• acc. to *Nyquist Theorem*…: the frequency span and the spectral resolution is related to the roof mirror travel

$$f_{max} = \frac{\omega_{max}}{2\pi} = \frac{1}{2 \cdot \Delta t} = \frac{c}{\Delta s} \qquad \Delta f = \frac{\Delta\omega}{2\pi} = \frac{1}{2 \cdot (t_{max} - t_{min})} = \frac{c}{\Delta s_{max} - s_{min}}$$

• keep in mind… MPI provides an auto-correlation measurement of radiation intensities → no phase information !!!

Reminder…: FEMTO Bunch Slicing – Longitudinal Bunch Distribution

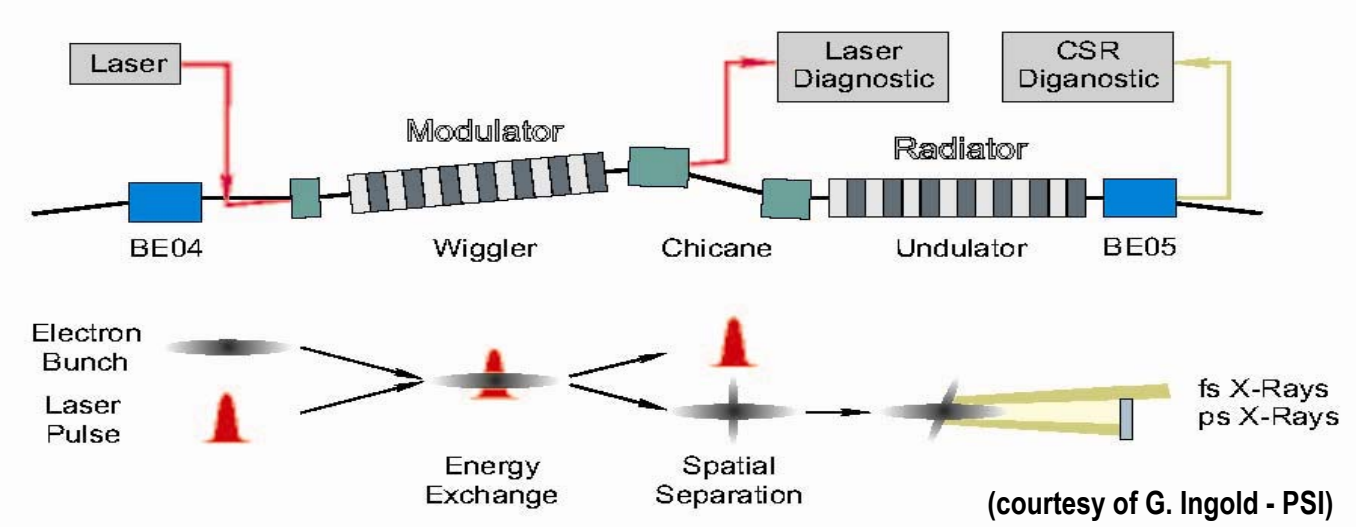

(courtesy of G. Ingold - PSI)

FEMTO-Bunch Slicing in SLS Storage Ring…:

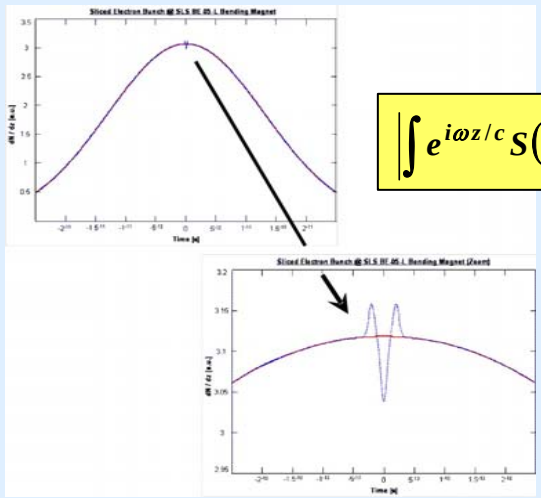

$$\left| \int e^{i\omega z/c} S(z) dz \right|^2$$

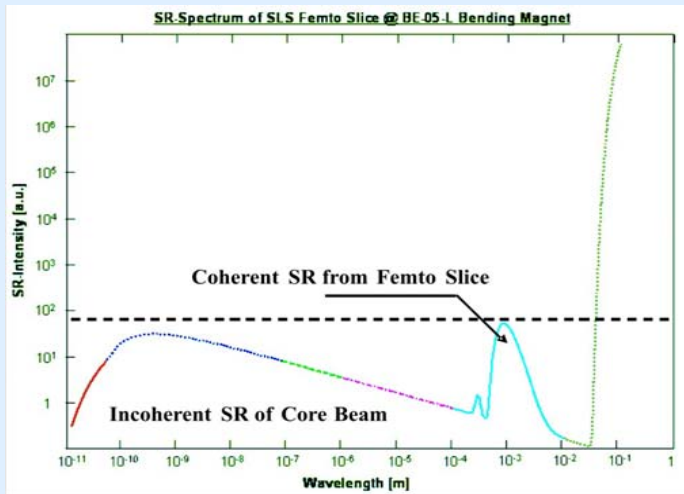

Coherent Radiation – Spectral Bunch Length Meas. from SLS FEMTO

prelim. data from: D. Abramsohn, Diploma thesis in preparation

Turn-by-Turn Long. Bunch Evolution after Bunch Slicing in SLS Storage Ring (Simulations by Davit Kalantarian (CANDLE))

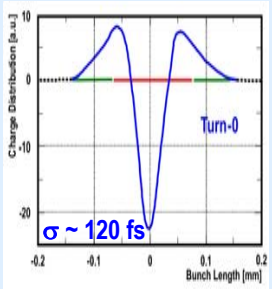

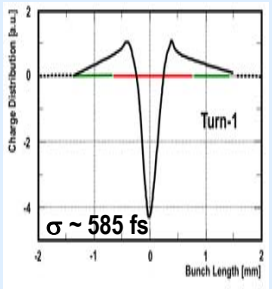

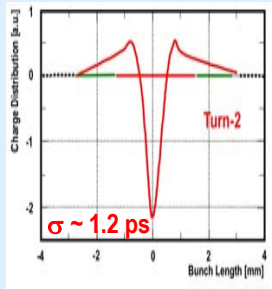

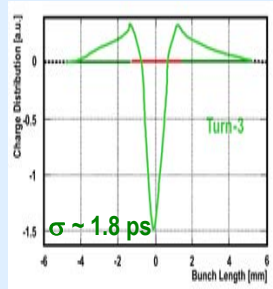

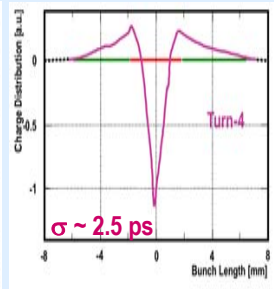

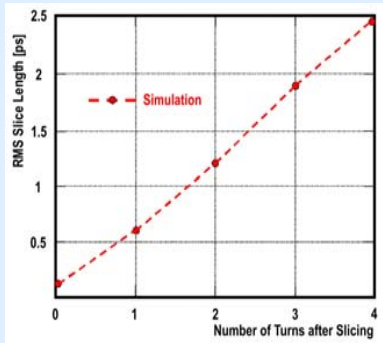

Notice: the scaling of the bunch length axis is increasing from ± 200 μm (turn-0) to ± 8 mm (turn-4)
storage ring revolution rate ~ 1 MHz → turn-by-turn revolution time ~ 1 μs

Integrated THz-Signal on InSb-Bolometer

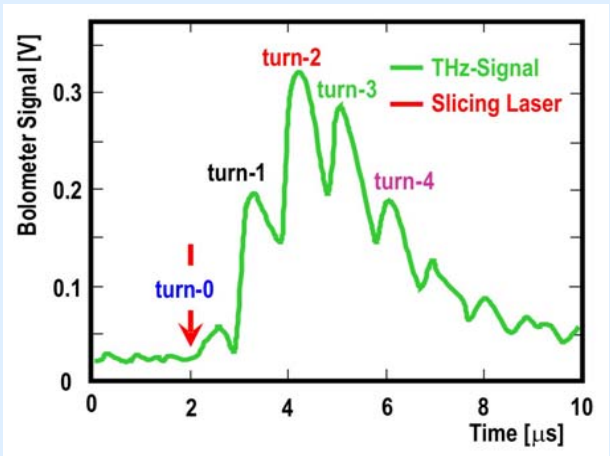

Spectral Intensities of Turns 0 – 4 (Simulations by D. Kalantarian (CANDLE))

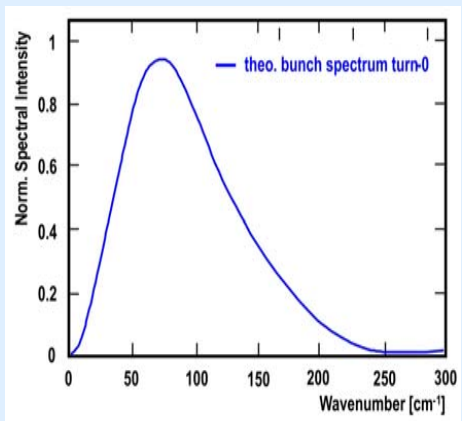

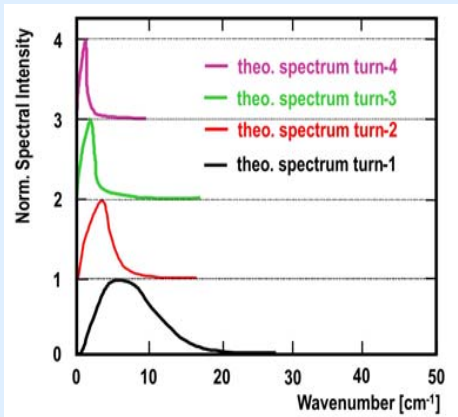

Coherent Radiation – Spectral Bunch Length Meas. from SLS FEMTO

Interferogramms from 5 consecutive turns after slicing

prelim. data from: D. Abramsohn, Diploma thesis in preparation

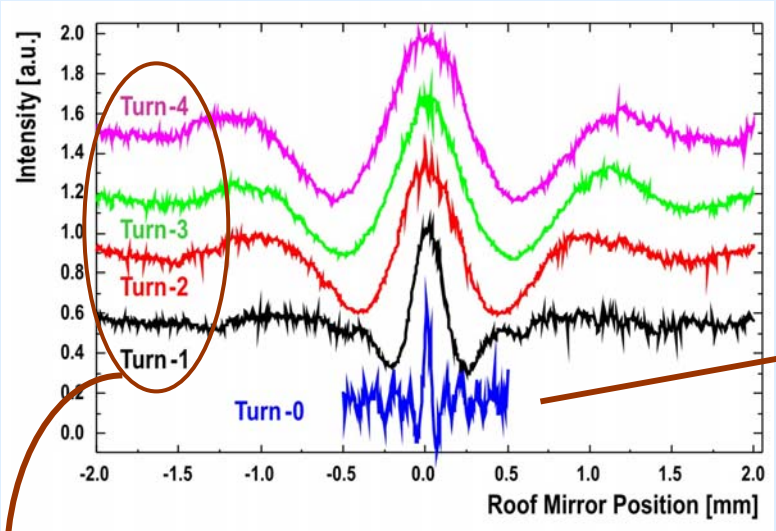

Spectral Intensity of Turn 0 (Theory and Experimental Data)

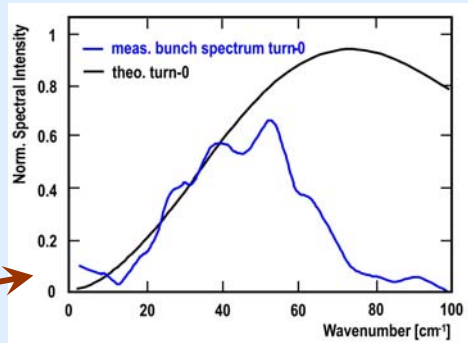

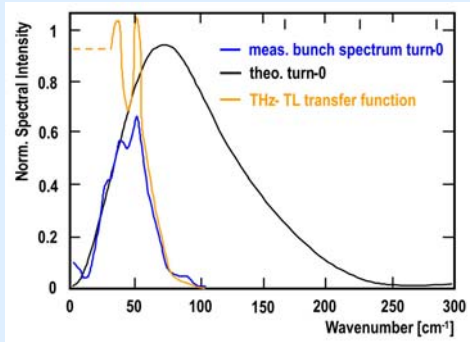

Spectral Intensities of Turns 1 to 4 after Slicing

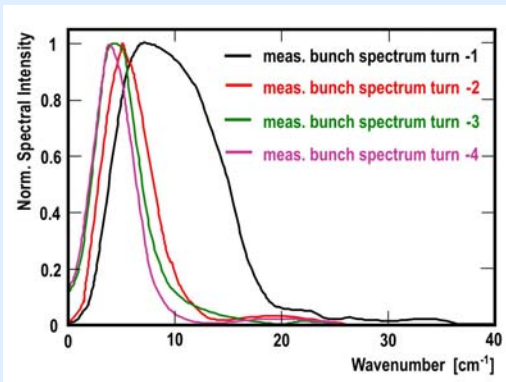

Bunch Lengths Evolution after Slicing in SLS Storage Ring

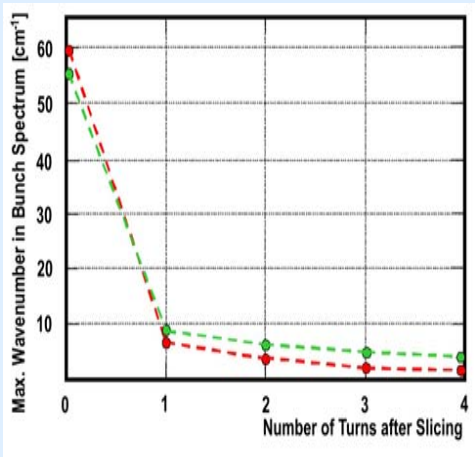

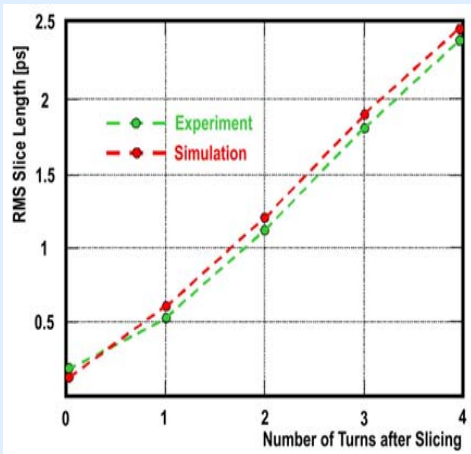

Bunch Lengths Determination by Spectroscopic Measurements – Flow Chart

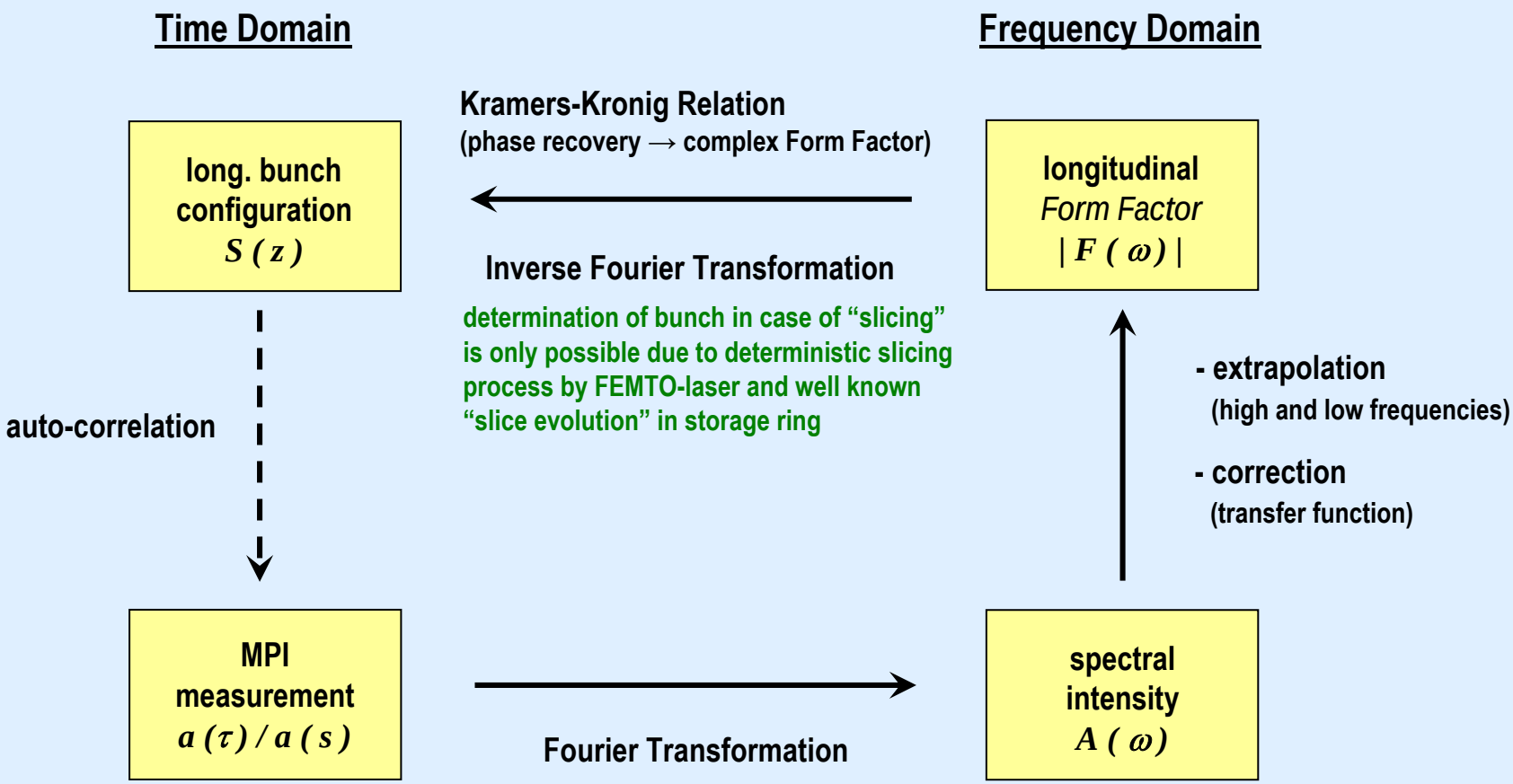

Bunch Lengths Determination by Spectroscopic Measurements

- intensity-based interferometry (MPI) reveals only the absolute value of the *Form Factor* → no phase information !

Symmetric Bunch Shapes

- for symmetric bunch configurations $S(z)$, the bunch *Form Factor* is retrieved from the coherent bunch spectrum by a cosine transform…:

$$F(\omega) = \left| \int e^{i\omega z/c} S(z) dz \right|^2 \quad \Rightarrow \quad S(z) = \frac{1}{\pi c} \int_0^\infty d\omega \sqrt{F(\omega)} \cdot \cos\left(\frac{\omega z}{c}\right)$$

Asymmetric Bunch Shapes and phase recovery by Kramers-Kronig Analysis…:

a well elaborated derivation of *Kramers-Kronig Relation* is given in: R. Lai, A.J. Sievers, NIM-A 397 (1997) 221 - 231

- the measured *Form Factor* $F(\omega)$ over the entire frequency spectrum provides directly the magnitude of the *Form Factor* amplitude $\rho(\omega)$…:

$$\rho(\omega) e^{i\psi(\omega)} \equiv \int_0^\infty S(z) e^{i\omega z/c} dz \qquad \text{and} \qquad \rho^2(\omega) = F(\omega)$$

- the *Form Factor* amplitude $\rho(\omega)$ is related to the long. bunch configuration by *inverse Fourier Transformation*…:

$$S(z) = \frac{1}{\pi c} \int_0^\infty d\omega \, \rho(\omega) \cdot \cos\left(\psi_m(\omega) - \frac{\omega z}{c}\right)$$

with the minimal phase… (retrieved by Kramers-Kronig relation)

$$\psi_m(\omega) = -\frac{2\omega}{\pi} \int_0^\infty \frac{\ln\left[\rho(x)/\rho(\omega)\right]}{x^2 - \omega^2} dx$$

- this formalism allows the recovery of asymmetric bunch structures – as usually produced in LINACs – but leaves the ambiguity of not being able to distinguish between a given bunch shape from the one flipped front to back

Bunch Lengths Determination by Spectroscopic Measurements

a well elaborated derivation of *Kramers-Kronig Relation* is given in: R. Lai, A.J. Sievers, NIM-A 397 (1997) 221 - 231

- intensity-based interferometry (MPI) reveals only the absolute value of the *Form Factor* → no phase information !

Symmetric Bunch Shapes

- for symmetric bunch configurations $S(z)$, the retrieval of the bunch *Form Factor* from the coherent bunch spectrum is achieved by a cosine transform…:

$$F(\omega) = \left| \int e^{i\omega z/c} S(z) dz \right|^2 \quad \Rightarrow \quad S(z) = \frac{1}{\pi c} \int_0^\infty d\omega \sqrt{F(\omega)} \cdot \cos\left(\frac{\omega z}{c}\right)$$

Asymmetric Bunch Shapes

- application of the *Kramers-Kronig analysis* provides the possibility to recover the missing phase information
- this formalism allows the recovery of asymmetric bunch structures – as usually produced in LINACs through bunch compression – but leaves the ambiguity of not being able to distinguish between a given bunch shape from the one flipped front to back
- in case of *FEMTO bunch slicing*, the bunch length and bunch shape is determined by the *slicing laser pulse*
  - → both laser pulse shape and pulse duration are known by laser auto-correlation measurements
  - → bunch evolution depends on storage ring optics, which is also well established and known

⇒ simulated bunch configurations can be fitted to measured bunch spectra

Bunch Lengths Determination by Spectroscopic Measurements – Overview

Time Domain

Frequency Domain

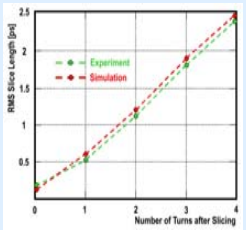

long. bunch configuration
$S(z)$

Kramers-Kronig Relation
(phase recovery → complex Form Factor)

Inverse Fourier Transformation

longitudinal
Form Factor
$|F(\omega)|$

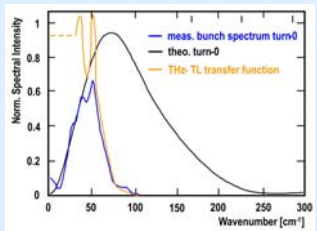

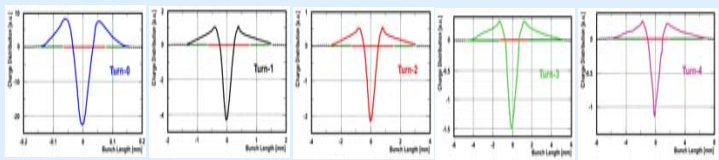

auto-correlation

- **extrapolation**
  (high and low frequencies)
- **correction**
  (transfer function)

MPI measurement
$a(\tau) / a(s)$

Fourier Transformation

spectral intensity
$A(\omega)$

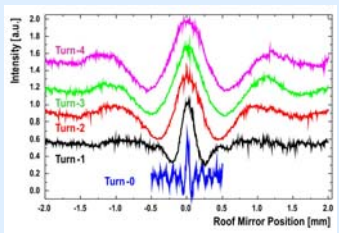

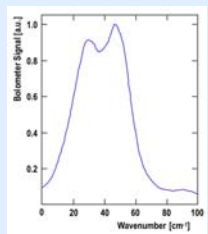

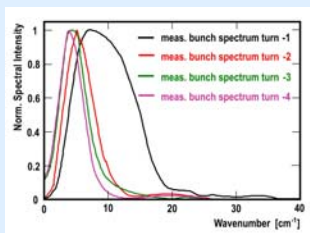

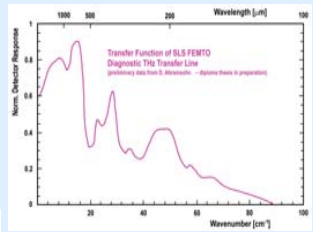

Single-Shot FIR Spectrometer – "Polychromator" (DESY approach, courtesy of B. Schmidt)

Schematic Set-Up of Single-Shot Spectrometer

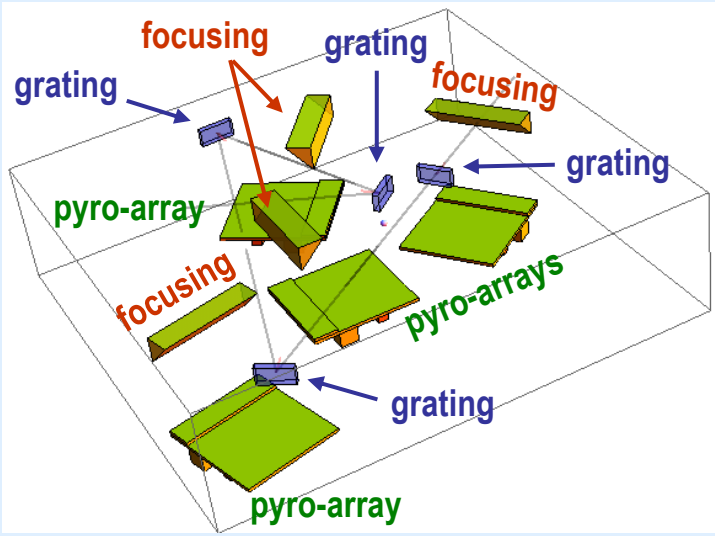

- single-shot spectrometer makes use of wavelength dependent reflection of gratings as dispersive elements
- one reflective blazed grating covers ~ 1.8 x base wavelength
  → four stages needed to cover one decade in a single-shot
- custom-made 30 channel pyro-detector array and fast, high-sensitivity readout unit (250 ns gating, 70 pC / channel)
- prelim. meas. show ultra short wavelength components
  → indicating very short bunch structures

Readout Module

30 Channel Pyro-Array

CTR Spectrum from FLASH bunches (raw data)

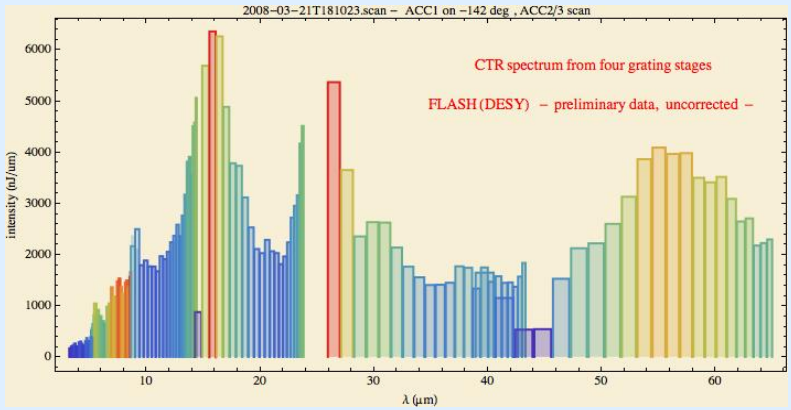

Summary of Spectroscopic Bunch Lengths Measurements

- the integrated intensity of coherent radiation emitted by short relativistic electron bunches provides a sensitive diagnostics ($I \sim N^2$) for bunching control and RF phase adjustment of accelerator structures
- Fourier spectroscopy using e.g.: Michelson or Martin-Puplett interferometers represents a robust and reliable method to determine the bunch *Form Factor* $F(\omega)$, which is proportional to the longitudinal bunch configuration $S(z)$
- there are basically no limitations towards the short wavelength regime, allowing to examine shortest bunch lengths and short-range structures within a bunch
- good knowledge about the measurement system transfer function is mandatory to reconstruct long. bunch shapes
- intensity-based interferomety reveals only the absolute value of the bunch *Form Factor* → no phase information !
- if the complete spectrum is known, recovery of phase information is possible through *Kramer-Kronig formalism*
- typically interferometric techniques average over many shots and provide only the *average long. bunch configuration*
- single-shot spectrometers have been designed and delivered good (preliminary) results…:
  - → see e.g.: Polychromator by Wanatabe et al., NIM-A 480 (2002) 315-327
  - → see e.g.: FLASH Single-Shot Spectrometer by H. Delsim-Hashemi et al., Proc. FLS, Hamburg 2006, WG512
  - → see e.g.: Spatial EO Auto-Correlation Interferometer by. D. Sütterlin et al., Proc. FEL'06, Stanford 2006, 648

EO Bunch Lengths Measurements – Introduction

- electro-optical detection inside the electron beam pipe (UHV-system) allows the direct measurement of the Coulomb field from highly relativistic electron bunches in the time domain
- the Coulomb field carried by short (sub-ps) electron bunches reaches – like coherent radiation – into the THz range
- the electric field induces a refractive index change in a birefringent crystal (e.g.: ZnTe, GaP), which is probed by a short pulse (fs), high bandwidth (some tens of nm) laser (linearly polarized, 800 – 1100nm)

Schematic Set-Up of EO Bunch Length Measurements

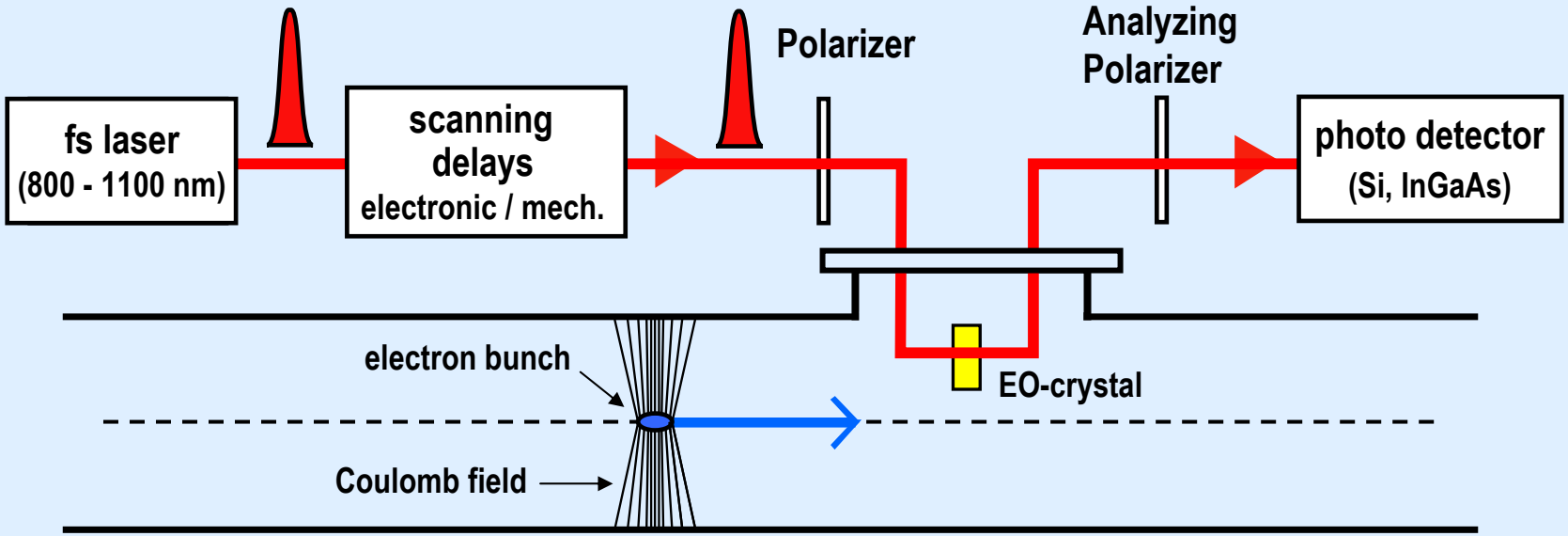

EO Bunch Lengths Measurements – Pockels Effect & EO-Detection

- an external electrical field (here: THz Coulomb field from the electron bunches) changes the refractive index of an optically active crystal (e.g.: ZnTe, GaP)…:

  → Polarization change as a function of field strength: $P = \varepsilon_0 \left(\chi_e^{(0)} E + \chi_e^{(1)} E^2 + \chi_e^{(2)} E^3 + \ldots \right)$

  $\chi_e^{(1)}$: Pockels effect; $\chi_e^{(2)}$: Kerr effect

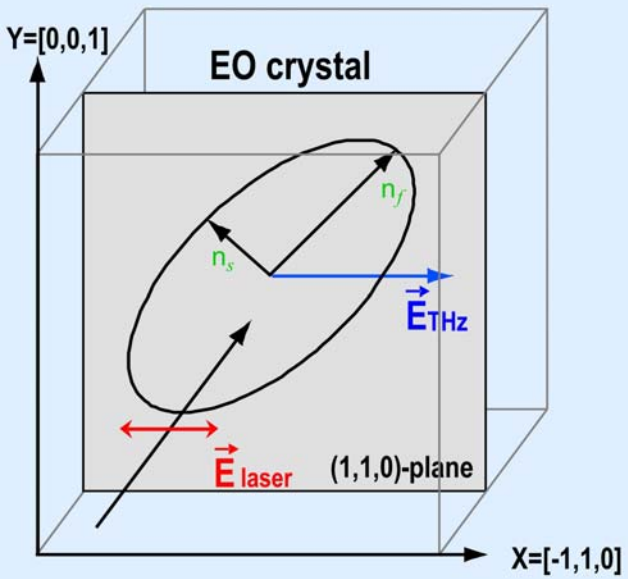

- the THz radiation E_{THz} passes the EO-crystal in the (1,1,0)-plane
- the two components of a linearly polarized probe laser pulse E_{laser} will see different refractive indices n_f and n_s in the crystal leading to a phase retardation and a subsequent polarization change (from linear to elliptical) of the laser pulse
- the phase retardation is proportional to the optical properties of the EO-crystal, the THz field strength and the crystal thickness..:

$$\Gamma_{max} = \frac{\omega d}{c}(n_1 - n_2) = \frac{\omega d}{c} E_{THz}\, n_0^3\, r_{41}$$

- a suitable arrangement of polarizers converts the ellipticity into an intensity modulation at the detector…:

  → cross polarizer arrangement: signal ~ Γ^2 → balanced detection: signal ~ Γ

EO Detection – Velocity Matching of THz and Optical Fields

- group and phase velocities of THz-waves in EO-crystals are frequency dependent and differ from each other leading to gradual distortion and lengthening of the THz-pulse over the crystal thickness
- lattice resonances (ZnTe at ~ 5 THz and GaP at ~ 11 THz) limit the EO response of a material
- laser pulse broadening is also visible due to phase retardation but can be neglected for thin crystals (< 200 μm)

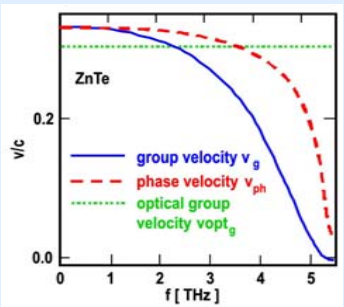

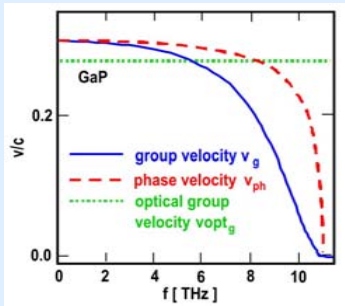

Propagation of THz and Laser Pulses through GaP

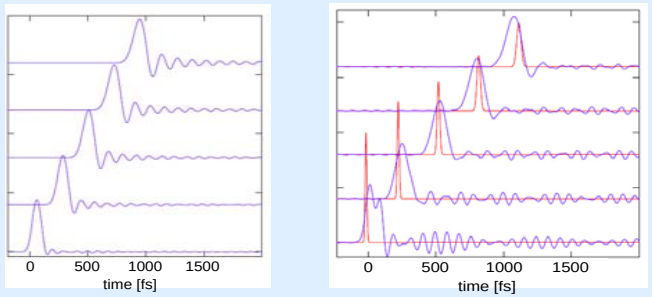

simulations by B. Steffen (DESY / PSI)

- EO response function depends mainly on material and crystal thickness

simulations by B. Steffen (DESY / PSI)

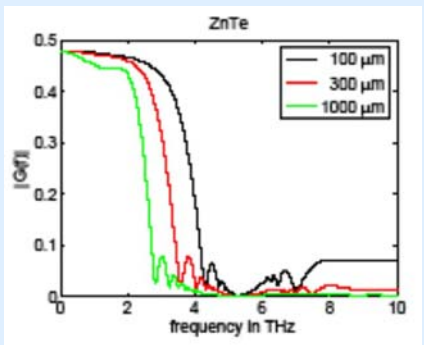

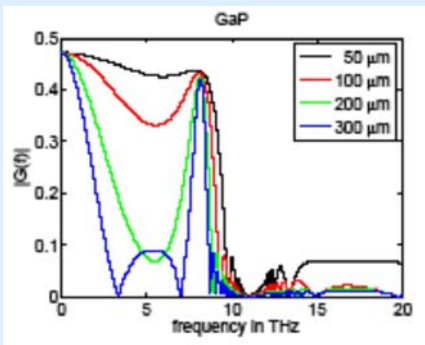

EO Detection – Probe Laser Options

- typically commercially available Ti:Sa lasers are used as probe lasers for EO readout
  - → providing short (few tens of fs) pulses with high bandwidth (some tens of nm)
  - → velocity matching @ 800 nm is fairly good
- new more compact and more stable Yb-doped fiber lasers are presently under development (e.g.: DESY and PSI)
  - → providing short (~ 50 fs) pulses with high bandwidth (some tens of nm) and superior amplitude stability
  - → superior velocity matching @ 1030 nm, which allows the use of thicker EO-crystals
  - → excellent synchronization to Er-doped fiber laser based optical master oscillators (~ 10 fs reference stability)

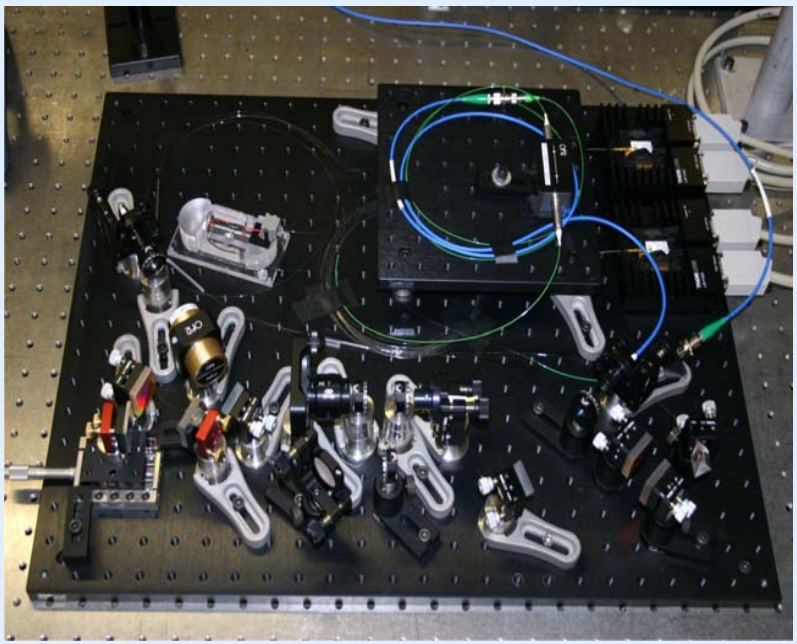

Yb-doped fiber laser system (oscillator and amplifier) by Felix Müller (PSI)

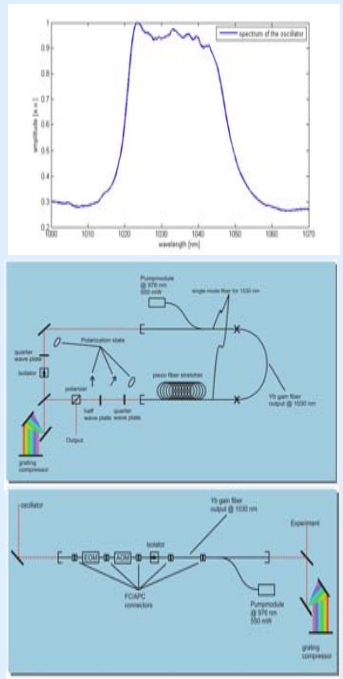

EO-response in GaP with Yb-doped fiber laser

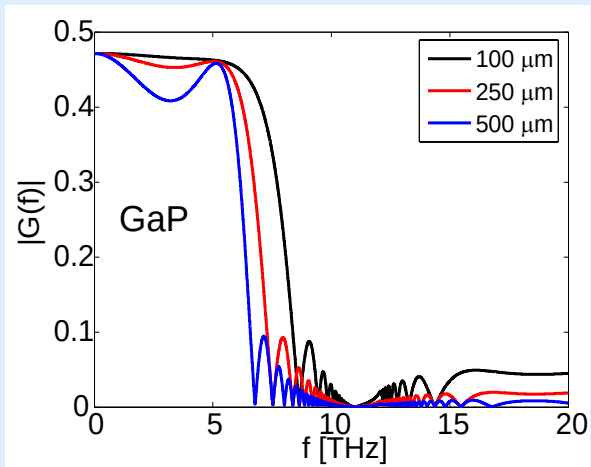

simulations by B. Steffen (DESY / PSI)

Electro-Optic Sampling

Schematic Set-Up of Electro-Optic Sampling with Variable Delay

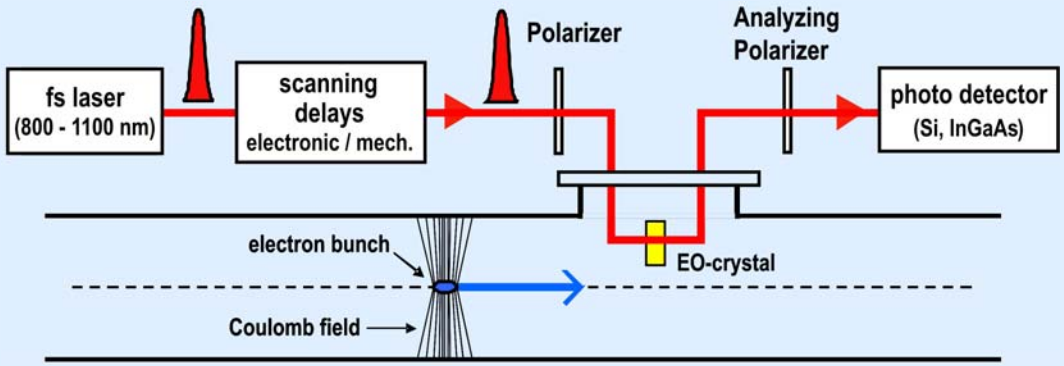

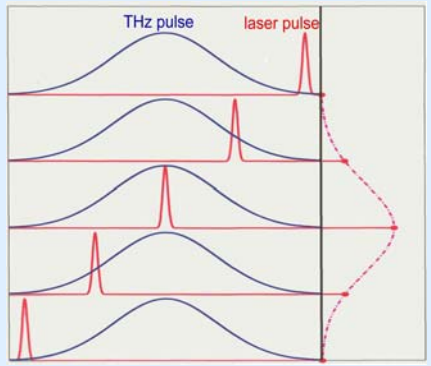

EOS Signal (outside UHV)

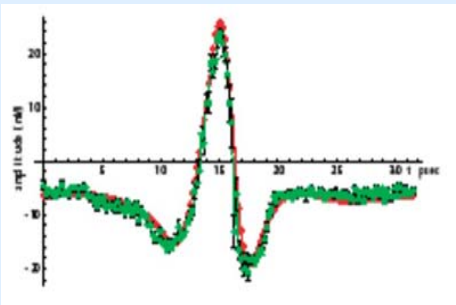

Bunch Reconstruction

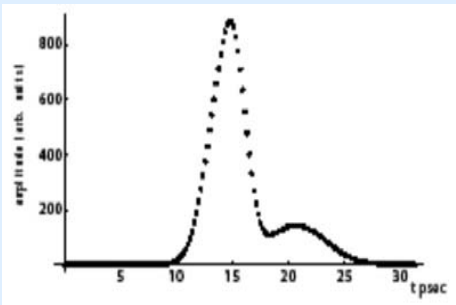

Meas. taken at SLS LINAC. See also: A. Winter et al., THOALH01, EPAC'04

EO-Sampling for fs Pulses

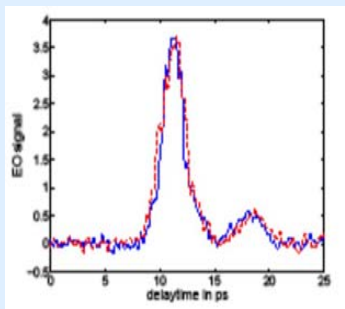

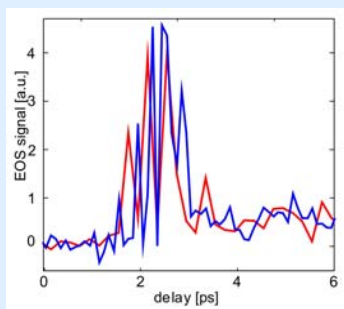

Meas. taken at FLASH. Courtesy of Bernd Steffen

- EO sampling is technically "simple" and provides high resolution (in the order of the laser pulse length)
- averaging over many bunches and limited by synchronization between laser and electron bunches

Spatially Resolved Electro-Optic Detection

Schematic Set-Up of Spatial Decoding

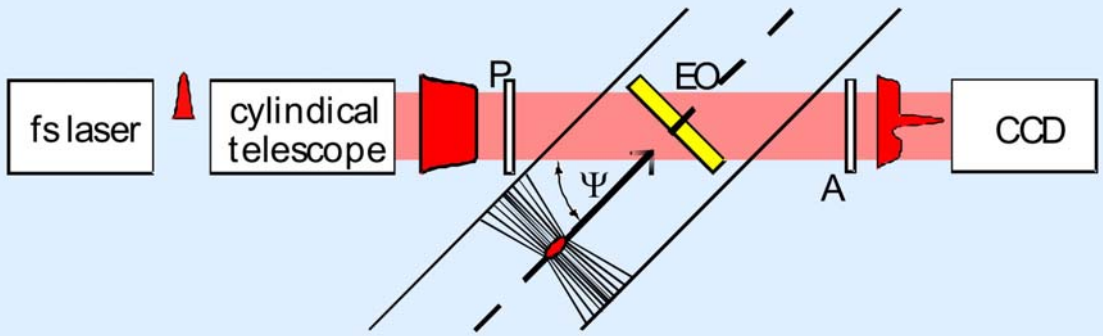

- similar approach like EO sampling but single-shot measurement
- temporal to spatial mapping through oblique incident between laser and Coulomb field in the plane above the laser and the EO-crystal
- angle ψ between laser and Coulomb field introduces a continuous time delay along the EO-crystal
- analyzer A turns spatial modulation of polarization into spatial intensity modulation, which is detected by a CCD camera
- requires spatially uniform laser beam and spatially uniform EO-crystal but stress induced birefringence prevents spatial uniformity in EO-crystals

Time Window

$$\Delta t = \frac{\Delta x}{c}\tan(\psi)$$

Δx - laser beam width

ψ - angle between laser and electron beam path

Example

$$\Delta t = \frac{3\cdot 10^{-3}\ m}{3\cdot 10^{8}\ ms^{-1}}\tan(45°) = 10\ ps$$

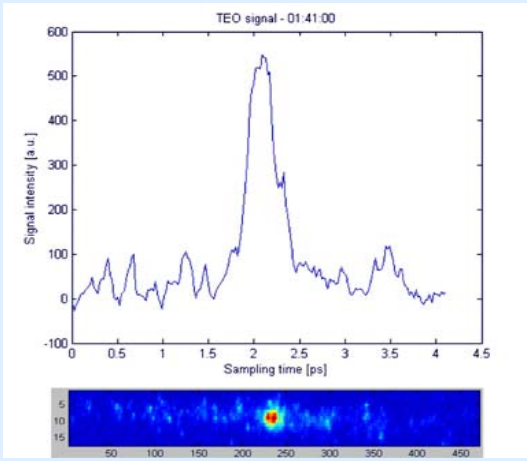

TEO measurement by A. Azima et al., DESY

Spectrally Resolved Electro-Optic Detection

Schematic Set-Up of Spectral Decoding

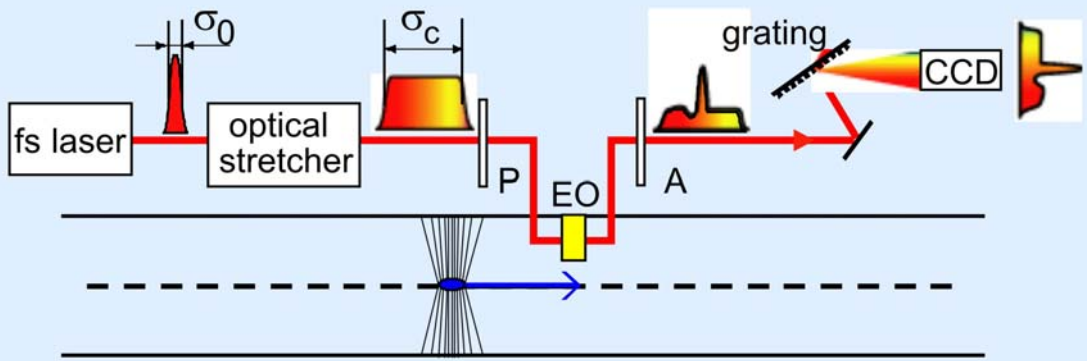

Time Resolution (Gaussian bunch shapes)

$$\sigma_{lim} \geq \sqrt{\sigma_0 \, \sigma_c}$$

σ_0 - laser beam duration

σ_c - chirped laser pulse duration

Example

$$\sigma_{lim} \geq \sqrt{7.5\ fs \cdot 1500\ fs} \geq 100\ fs$$

- EO spectral decoding is a single-shot measurement
- linear chirp is encoded on the laser pulse by passing a dispersive material or grating stretcher
- chirped laser pulse travels in parallel to the Coulomb field through EO-crystal encoding a frequency-time correlation onto the laser spectrum
- analyzer A turns modulation of polarization into an intensity modulation, which is sent through a spectrometer and measured by a CCD camera
- laser pulse energy spread over many pixel → higher laser pulse energy
- frequency mixing of THz wave and laser distorts frequency-time correlation

Spectral Decoding (GaP 175 µm, σ_0 = 7 fs, σ_c = 1.5 ps)

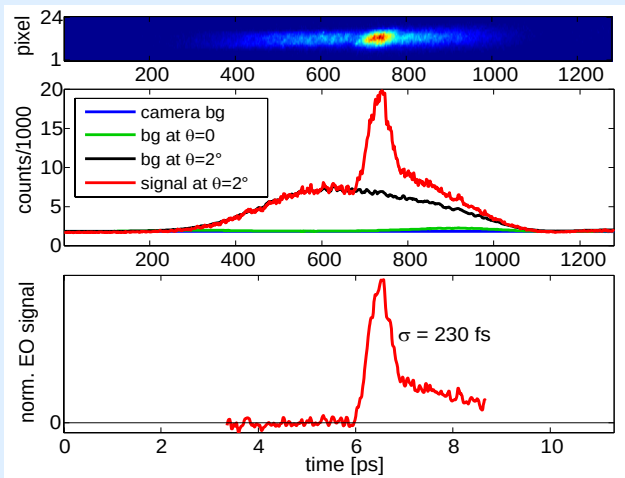

measurement by B. Steffen et al., DESY

Temporally Resolved Electro-Optic Detection

Schematic Set-Up of Temporal Decoding

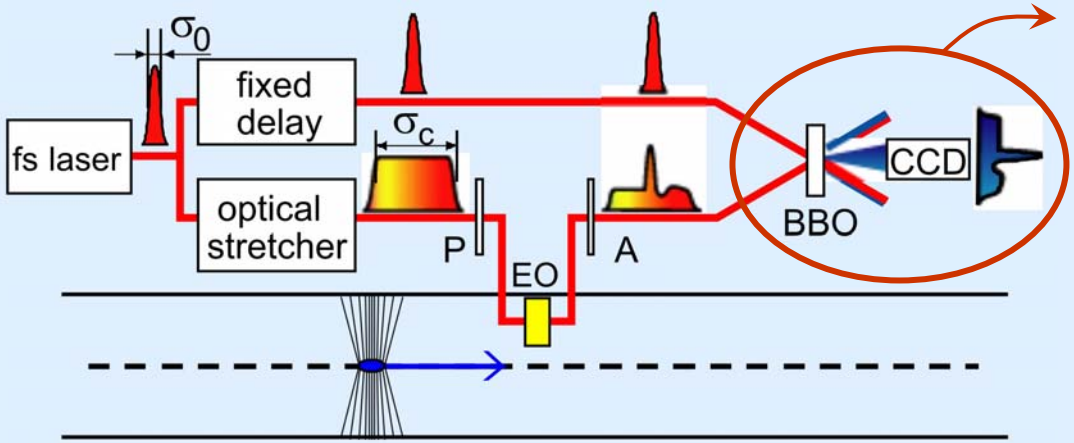

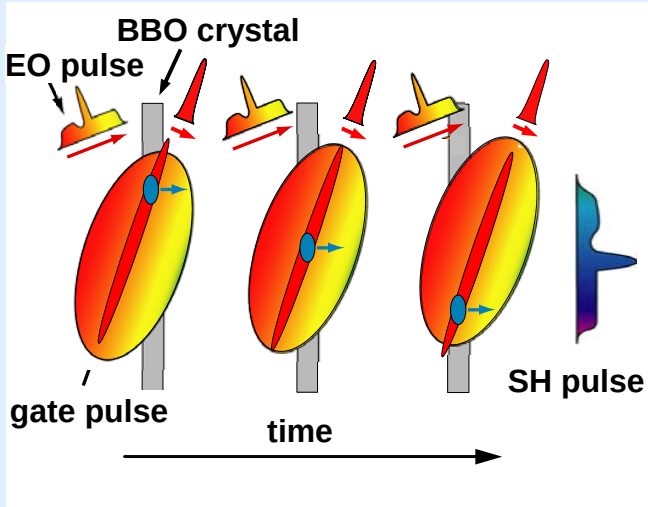

- EO temporal decoding is a single-shot measurement, where the chirped laser pulse travels in parallel to the Coulomb field through the EO-crystal encoding a frequency-time correlation onto the probe laser spectrum
- the analyzer A turns the modulation of polarization into an intensity modulation
- SH light is generated by cross-correlating the modulated EO-pulse and the short laser pulse in a BBO-crystal
- the SH-generation in the BBO-crystal works similar to the spatial decoding technique and is proportional to the square of the incoming intensities: $I_{SH} \sim I_{gate} \cdot I_{EO}$
- using a 300 μm thick BBO-crystal and a 30 fs gate pulse, a time resolution of < 100 fs can be reached
- due to the low efficiency of the SH-process, a pulse energy of 100 μJ from an amplified laser system is required

Temporally Resolved Electro-Optic Detection

Measurement of FLASH Bunches with EOTD *

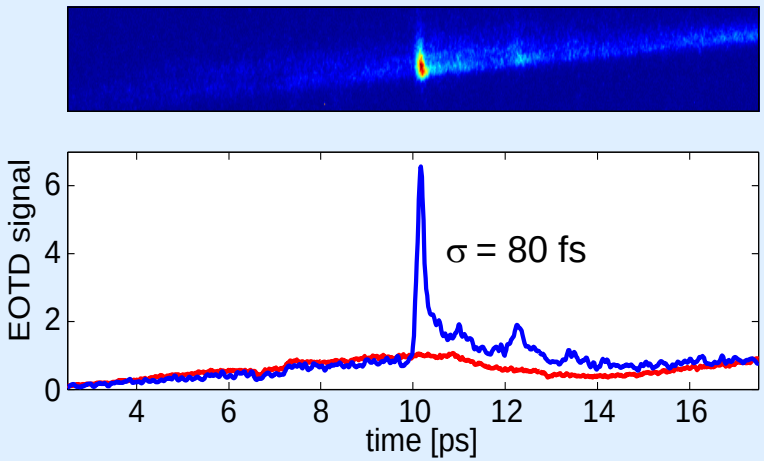

Comparison between EOTD and Transverse Deflector *

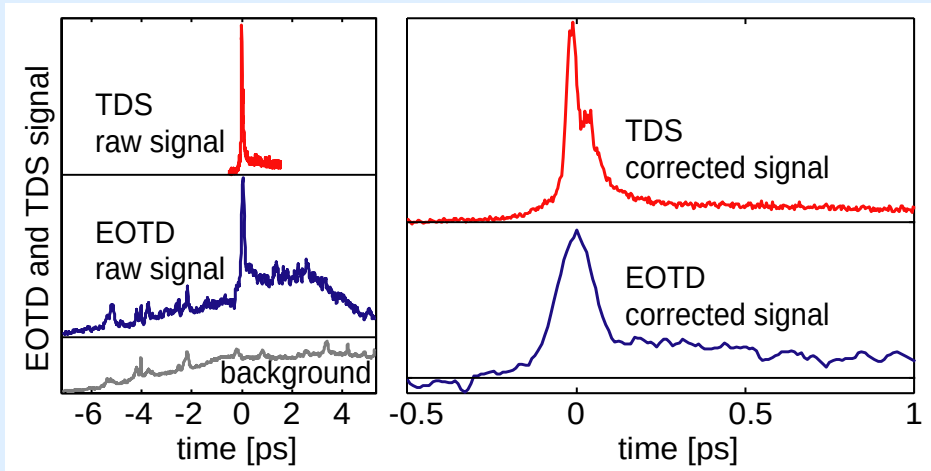

electron bunch lengths as short as 55 fs have been measured with temporally resolved EO detection!

(This is close to the resolution limit of GaP)

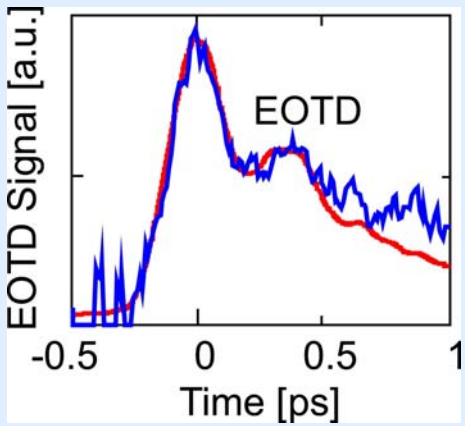

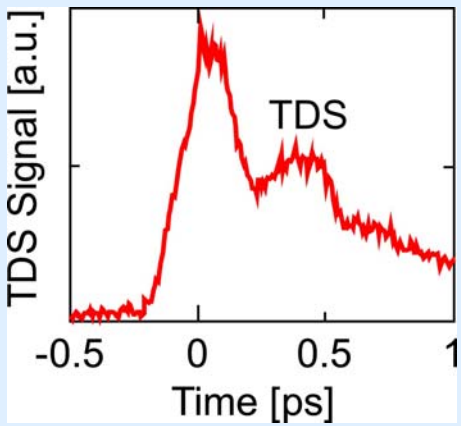

* EOTD measurements by B. Steffen et al., DESY,
see also: B. Steffen, DESY-thesis-2007-020, July 2007
TDS measurements by M. Roehrs, DESY

Set-Ups of Temporal and Spectral Decoding in FLASH Accelerator Tunnel

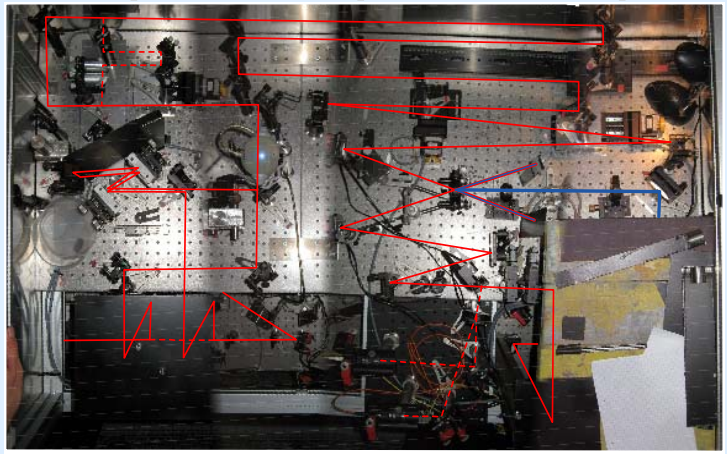

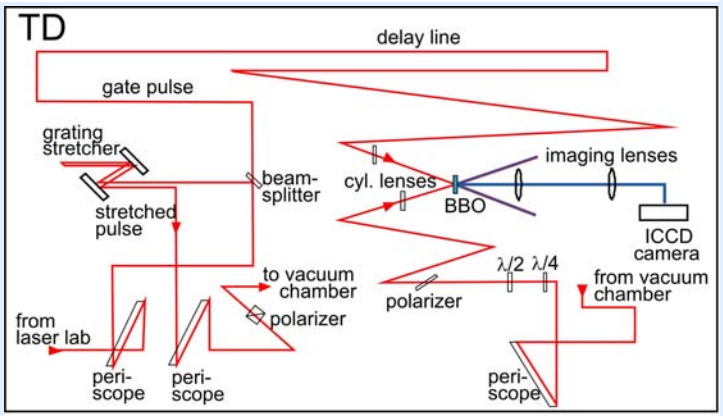

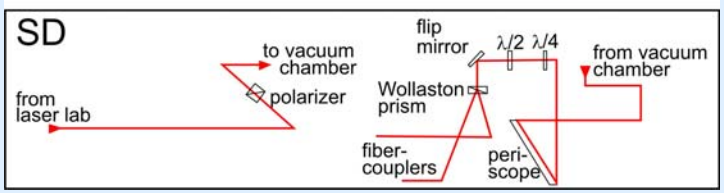

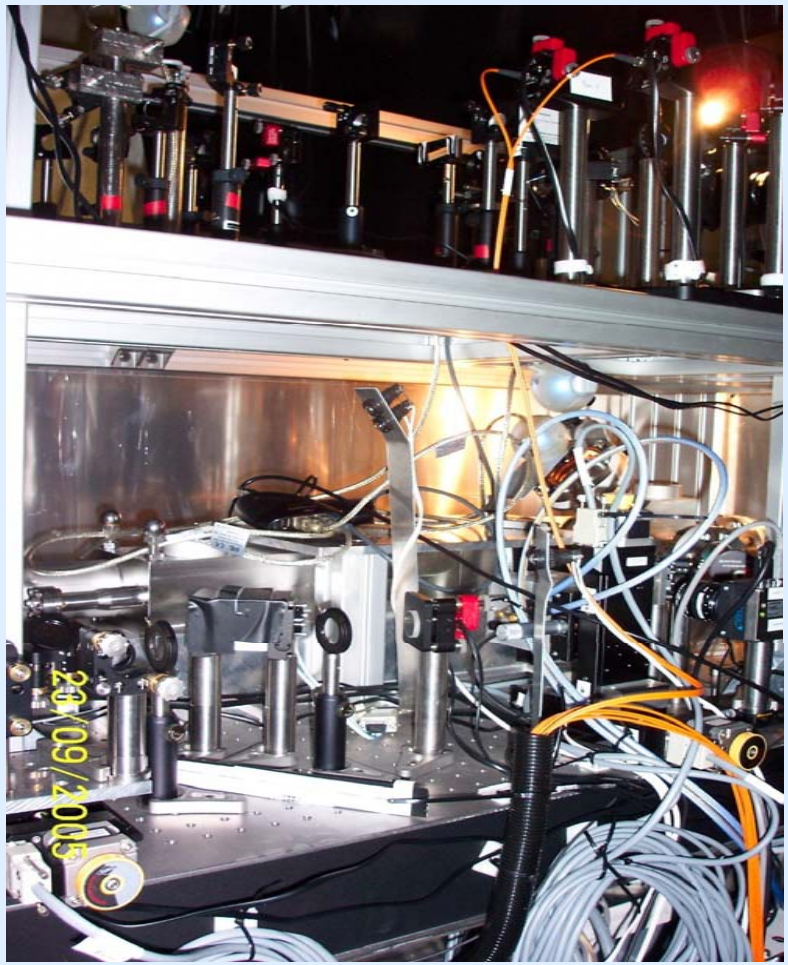

all images taken from B. Steffen, DESY-thesis-2007-020, July 2007

Electro-Optical Bunch Arrival Time Monitor – FLASH Design

Principle of EO Bunch Arrival Time Monitor (FLASH-design)

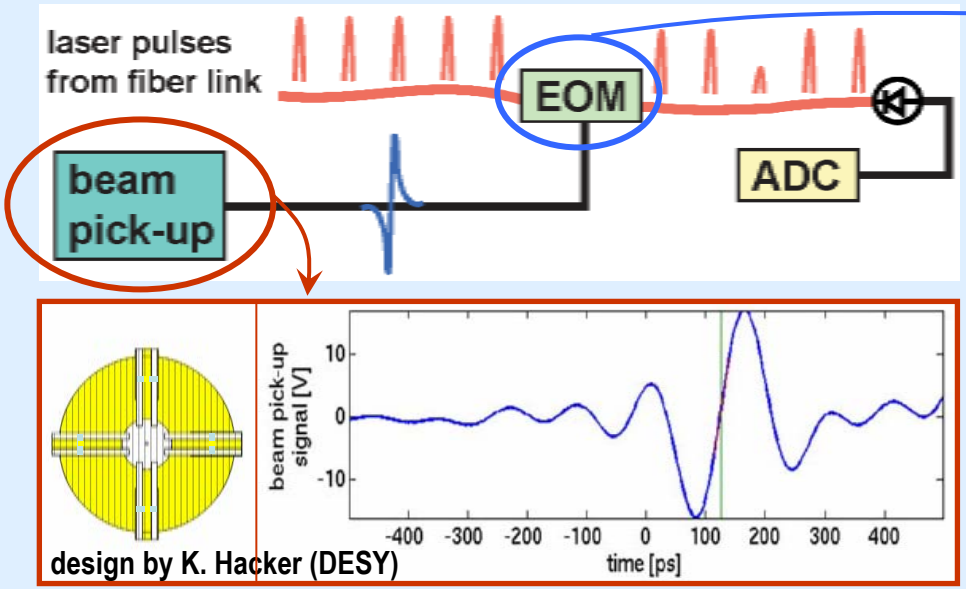

Commercial EO Modulator (10 – 40 GHz BW)

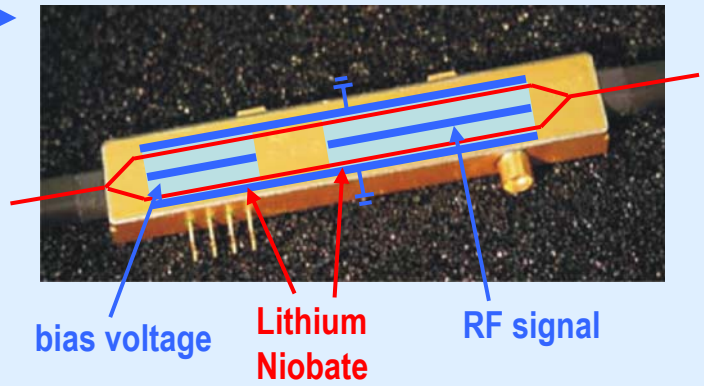

Electro-Optical BAM Measurement Principle

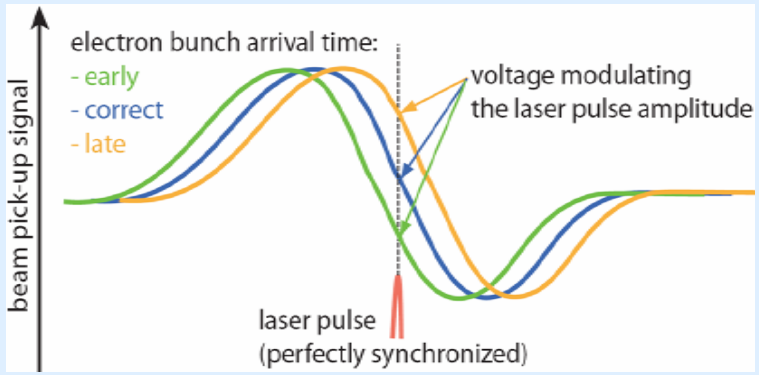

images and measurements taken from F. Löhl et al., DESY

EO BAM Resolution (~ 10 fs)

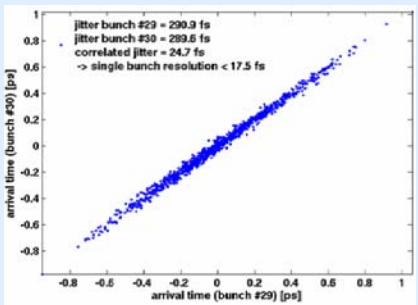

BAM Correction on FLASH Beam

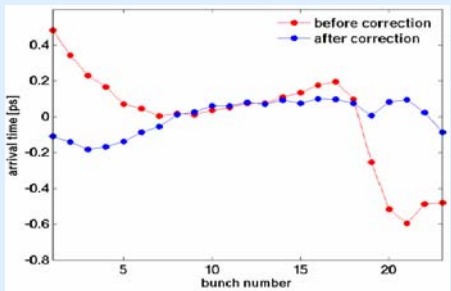

Femto-Second Diagnostics – Summary (personal opinion…)

various measurement techniques in the *Time Domain* and *Spectral Domain* have been developed and presented…

Time Domain:

fs streak cameras…:
- → provide sub-ps (> 300 fs) time resolution for quasi monochromatic visible light
- → very useful for optimization of gun laser profile and low energy electron beam

but quite limited time resolution and does not provide "feedback-usable" signals

transv. RF deflectors…:
- → provide excellent (~ 10 fs) time resolution by deflecting directly the particle beam
- → very versatile diagnostic for time resolved measurement of transverse and longitudinal phase space (sliced emittances and energy distribution)
- → unfortunately destructive measurement method

EO techniques…:
- → provide excellent (> 50 fs) time resolution by measuring the beam's Coulomb field
- → spatial, spectral and temporal decoding are single-shot methods, which measure the bunch length and provide high resolution (~ 10 fs) beam arrival time information
- → unfortunately still very complex (optical) set-ups using (high power) fs lasers

Spectral Domain

Interferometers…:
- → interferometric meas. are very robust and provide excellent spectral (temporal) resolution
- → single-shot measurements have been accomplished
- → transfer functions have to be known and phase information is usually not available